Inorganic Chemistry

Article

pubs.acs.org/IC

Preparation and Redox Studies of α_1- and α_2-Isomers of Mono-Ru-Substituted Dawson-type Phosphotungstates with a DMSO Ligand: $[\alpha_1/\alpha_2\text{-}P_2W_{17}O_{61}Ru^{II}(DMSO)]^{8-}$

Shuhei Ogo,[†] Noriko Shimizu,[†] Kensuke Nishiki,[†] Nobuhiro Yasuda,[‡] Tsutomu Mizuta,[§] Tsuneji Sano,[†] and Masahiro Sadakane*[,†,∥]

[†]Department of Applied Chemistry, Graduate School of Engineering, Hiroshima University, 1-4-1 Kagamiyama, Higashi-Hiroshima 739-8527, Japan

[‡]Japan Synchrotron Radiation Research Institute/SPring-8, 1-1-1 Kouto, Sayo-cho, Sayo-gun, Hyogo 679-5198, Japan

[§]Department of Chemistry, Graduate School of Science, Hiroshima University, 1-3-1 Kagamiyama, Higashi-Hiroshima 739-8527, Japan

[∥]PRESTO, Japan Science and Technology Agency (JST), 4-1-8 Honcho, Kawaguchi, Saitama 332-0012, Japan

Supporting Information

ABSTRACT: Both α_1- and α_2-isomers of mono-Ru-substituted Dawson-type heteropolytungstates with a DMSO ligand, $[\alpha_1\text{-}P_2W_{17}O_{61}Ru^{II}(DMSO)]^{8-}$ and $[\alpha_2\text{-}P_2W_{17}O_{61}Ru^{II}(DMSO)]^{8-}$, are prepared from the α_2-isomer of a monolacunary derivative, $[\alpha_2\text{-}P_2W_{17}O_{61}]^{10-}$. Reaction of $[\alpha_2\text{-}P_2W_{17}O_{61}]^{10-}$ with $Ru(DMSO)_4Cl_2$ under hydrothermal conditions produces $[\alpha_2\text{-}P_2W_{17}O_{61}Ru^{II}(DMSO)]^{8-}$ as a main product together with $[\alpha_1\text{-}P_2W_{17}O_{61}Ru^{II}(DMSO)]^{8-}$, $[PW_{11}O_{39}Ru^{II}(DMSO)]^{5-}$, and $[P_2W_{18}O_{62}]^{6-}$ as byproducts. By addition of KCl to the reaction mixture, $K_8[\alpha_2\text{-}P_2W_{17}O_{61}Ru^{II}(DMSO)]$ is isolated in a moderate yield. On the other hand, reaction of $[\alpha_2\text{-}P_2W_{17}O_{61}]^{10-}$ with $Ru_2(benzene)_2Cl_4$ under hydrothermal conditions produces an isomeric mixture of $[P_2W_{17}O_{61}Ru^{III}(H_2O)]^{7-}$ (α_1-isomer/α_2-isomer ratio: ca. 8/1) as a main product together with $[PW_{11}O_{39}Ru^{III}(H_2O)]^{4-}$ and $[P_2W_{18}O_{62}]^{6-}$ as byproducts. By addition of acetone to the reaction mixture, $K_7[P_2W_{17}O_{61}Ru^{III}(H_2O)]$ is isolated in a good yield. Reaction of $[P_2W_{17}O_{61}Ru^{III}(H_2O)]^{7-}$ with DMSO produces $[\alpha_1\text{-}P_2W_{17}O_{61}Ru^{III}(DMSO)]^{7-}$ as a main product and $[\alpha_2\text{-}P_2W_{17}O_{61}Ru^{III}(DMSO)]^{7-}$ as a minor product. By addition of KCl and acetone, the α_1-isomer $K_8[\alpha_1\text{-}P_2W_{17}O_{61}Ru^{II}(DMSO)]$ is isolated in a good yield. Both compounds are fully analyzed by CV, NMR (^1H, ^{13}C, ^{31}P, and ^{183}W), IR, UV–vis, elemental analysis, mass spectroscopy, and single-crystal structure analysis. Assuming that isomerization does not occur during the reaction of $[P_2W_{17}O_{61}Ru^{III}(H_2O)]^{7-}$ with DMSO, the isolated $[P_2W_{17}O_{61}Ru^{III}(H_2O)]^{7-}$ contains the α_1-isomer as a main compound with the α_2-isomer as a minor compound. Unusual transformation of the α_2-isomer of $[P_2W_{17}O_{61}]^{10-}$ to the α_1-isomer occurs. Redox behaviors of $[\alpha_1\text{-}P_2W_{17}O_{61}Ru^{II}(DMSO)]^{8-}$ and $[\alpha_2\text{-}P_2W_{17}O_{61}Ru^{II}(DMSO)]^{8-}$ are compared together with Ru(DMSO)-substituted α-Keggin-type heteropolytungstates, $[\alpha\text{-}XW_{11}O_{39}Ru(DMSO)]^{n-}$ (X = Si, Ge, and P).

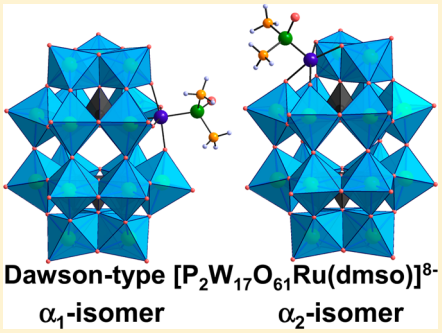

INTRODUCTION

Polyoxometalates (POMs) are discrete metal-oxide clusters of W, Mo, V, and Nb that have been attracting increasing interest because of their multielectronic redox activities, photochemical properties, acidic properties, and magnetic properties, resulting in potential applications of POMs as catalysts and functional materials.[1−3] Recently, considerable attention has been directed toward monoruthenium (Ru)-substituted Keggin-type heteropolytungstates because of the unique redox and catalytic properties of the Ru atom.[4,5] Catalytic activities of mono-Ru-substituted heteropolytungstates for the oxidation of cyclooctene,[6] water,[7−9] and alcohols[10,11] and the reduction of dimethyl sulfoxide (DMSO)[12] and carbon dioxide[13] have been reported.

In the course of our research on mono-Ru-substituted polyoxometalates, we have reported preparation and structural characterization of various mono-ruthenium-substituted α-Keggin-type heteropolytungstates with a terminal aqua ligand, $[\alpha\text{-}XW_{11}O_{39}Ru^{III}(H_2O)]^{n-}$, (X = Si ($n$ = 5), Ge (n = 5), and P (n = 4)),[8,14,15] and with a DMSO ligand, $[\alpha\text{-}XW_{11}O_{39}Ru\text{-}(DMSO)]^{n-}$ (X = Si, Ge, and P).[9,15,16] The complexes with a terminal aqua ligand, $[\alpha\text{-}XW_{11}O_{39}Ru^{III}(H_2O)]^{n-}$ (X = Si (n = 5), Ge (n = 5), and P (n = 4)), were prepared by reactions of monolacunary heteropolytungstates, $[XW_{11}O_{39}]^{n-}$ (X = Si (n = 8), Ge (n = 8), and P (n = 7)), with $Ru(acac)_3$ (acac: acetylacetonate) or $Ru_2(benzene)_2Cl_4$ under hydrothermal

Received: December 10, 2013
Published: March 10, 2014

   dx.doi.org/10.1021/ic403041s | Inorg. Chem. 2014, 53, 3526−3539

conditions (eq 1).[8,14] Two DMSO-coordinated complexes, $[\alpha\text{-}XW_{11}O_{39}Ru^{III}(DMSO)]^{5-}$ (X = Si or Ge), were produced by reaction of water-coordinated complexes $[\alpha\text{-}XW_{11}O_{39}Ru^{III}(H_2O)]^{5-}$ (X = Si or Ge), with DMSO (eq 2),[15,16] and the phosphorus derivative $[\alpha\text{-}PW_{11}O_{39}Ru^{II}(DMSO)]^{5-}$ was produced by a reaction of monolacunary heteropolytungstates, $[PW_{11}O_{39}]^{7-}$, with $Ru(DMSO)_4Cl_2$ under hydrothermal conditions (eq 3).[9]

$$[\alpha\text{-}XW_{11}O_{39}]^{n-} + Ru(acac)_3 \text{ or } Ru_2(benzene)_2Cl_4 \rightarrow [\alpha\text{-}XW_{11}O_{39}Ru^{III}(H_2O)]^{(n-3)-} \text{ (X = Si } (n = 8), \text{ Ge } (n = 8), \text{ or P } (n = 7)) \quad (1)$$

$$[\alpha\text{-}XW_{11}O_{39}Ru^{III}(H_2O)]^{5-} + DMSO \rightarrow [\alpha\text{-}XW_{11}O_{39}Ru^{III}(DMSO)]^{5-} \text{ (X = Si or Ge)} \quad (2)$$

$$[\alpha\text{-}PW_{11}O_{39}]^{7-} + Ru(DMSO)_4Cl_2 \rightarrow [\alpha\text{-}PW_{11}O_{39}Ru^{II}(DMSO)]^{5-} \quad (3)$$

As in the case of α-Keggin-type heteropolytungstates, Dawson-type heteropolytungstate, $[P_2W_{18}O_{62}]^{6-}$, can incorporate another metal. There are two kinds of tungstens, so-called "cap" and "belt" tungstens, and removal of the belt or cap tungsten results in formation of the α_2-isomer or α_1-isomer of a monolacunary compound, $[P_2W_{17}O_{61}]^{10-}$, respectively (Figure 1). Incorporation of Ru in this vacancy to form α_1- or α_2-isomers of mono-Ru-substituted Dawson-type heteropolytungstates, $[P_2W_{17}O_{61}Ru(L)]^{(10-n)-}$ (L: ligand, n = valence of Ru), is highly desired for the following reasons: (1) It is expected that redox potentials of Ru in Dawson-type heteropolytungstates are different from those in Keggin-type heteropolytungstates, and different redox activities are expected. (2) Two phosphorus atoms in the molecule are detectable by ^{31}P NMR, and analysis of the compound during not only preparation procedures but also catalytic reactions using ^{31}P NMR is possible. (3) The α_1-isomer is an enantiomer, though it usually exists as a racemic mixture, and after enantiomer separation, the α_1-isomer has potential as an all-inorganic enantioselective redox mediator and enantioselective sensor.[17−19]

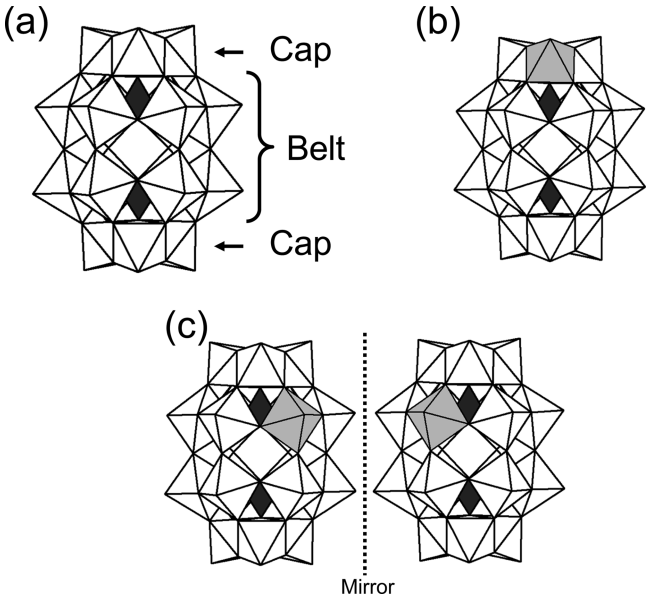

Figure 1. Polyhedral presentations of (a) a Dawson-type phosphotungstate, $[\alpha\text{-}P_2W_{18}O_{62}]^{6-}$, and (b) α_2-isomer and (c) α_1-isomer of a monometal-substituted Dawson-type phosphotungstate, $[P_2W_{17}O_{61}M]^{n-}$. White, black, and gray polyhedra represent WO_6 octahedron, PO_4 tetrahedron, and MO_5L (M, substituted metal; L, ligand) octahedron, respectively.

However, preparation of mono-Ru-substituted Dawson-type heteropolytungstates in pure form has not yet been achieved. Pope's group reported synthesis of mono-Ru-substituted α_2-Dawson-type heteropolytungstate, $[\alpha_2\text{-}P_2W_{17}O_{61}Ru^{III}(H_2O)]^{7-}$, by a reaction of $[\alpha_2\text{-}P_2W_{17}O_{61}]^{10-}$ with $[Ru(H_2O)_6](C_7H_7SO_3)_2$.[12] Nomiya's group reported synthesis of $[\alpha_2\text{-}P_2W_{17}O_{61}Ru^{III}(H_2O)]^{7-}$ by a reaction of $[\alpha_2\text{-}P_2W_{17}O_{61}]^{10-}$ with $Ru(DMSO)_4Cl_2$ followed by oxidation with Br_2.[20] However, both groups reported that the obtained compound was not pure but a mixture with $[P_2W_{18}O_{62}]^{6-}$. Furthermore, synthesis of the α_1-isomer, $[\alpha_1\text{-}P_2W_{17}O_{61}Ru(L)]^{n-}$ (L = ligand), has never been reported.

In this Article, we describe synthesis and isolation of both α_1- and α_2-isomers of mono-Ru-substituted Dawson-type heteropolytungstates with a DMSO ligand, $[\alpha_1/\alpha_2\text{-}P_2W_{17}O_{61}Ru(DMSO)]^{8-}$. Surprisingly, the α_1-isomer was prepared from the α_2-isomer of the monolacunary starting compound, $[\alpha_2\text{-}P_2W_{17}O_{61}]^{10-}$. Usually, the α_1-isomer is less stable than the α_2-isomer, and the α_1-isomer should be produced from $[\alpha_1\text{-}P_2W_{17}O_{61}]^{10-}$ under controlled conditions.[17] Redox behaviors of $[\alpha_1\text{-}P_2W_{17}O_{61}Ru(DMSO)]^{n-}$ and $[\alpha_2\text{-}P_2W_{17}O_{61}Ru(DMSO)]^{n-}$ are compared together with α-Keggin-type derivatives, $[\alpha\text{-}XW_{11}O_{39}Ru(DMSO)]^{n-}$ (X = Si, Ge, or P).

EXPERIMENTAL SECTION

Materials. Homemade deionized water (Millipore, Elix) was used. The compounds $K_{10}[\alpha_2\text{-}P_2W_{17}O_{61}]\cdot 15H_2O$ (no $[\alpha_1\text{-}P_2W_{17}O_{61}]^{10-}$ detected by ^{31}P NMR), $K_9Li[\alpha_1\text{-}P_2W_{17}O_{61}]\cdot 15H_2O$ (no $[\alpha_2\text{-}P_2W_{17}O_{61}]^{10-}$ detected by ^{31}P NMR) (Supporting Information Figure S1a−c), and $Ru(DMSO)_4Cl_2$ were prepared according to the published procedure and analyzed by ^1H NMR, ^{31}P NMR, and/or IR spectroscopy.[21,22] All other chemicals were reagent-grade and used as supplied.

Preparation of $K_8[\alpha_2\text{-}P_2W_{17}O_{61}Ru^{II}(DMSO)]\cdot 16H_2O$. $Ru(DMSO)_4Cl_2$ (0.04 g, 0.083 mmol), $K_{10}[\alpha_2\text{-}P_2W_{17}O_{61}]\cdot 15H_2O$ (0.39 g, 0.083 mmol), and water (5 mL) were poured into a 50 mL Teflon-liner autoclave and bubbled with nitrogen for 30 min (pH of the solution was 6.6). Afterward, the autoclave was placed in a conventional oven heated at 140 °C for 5 h. After the autoclave had been cooled to room temperature, the reaction mixture was filtered. Subsequently, KCl (0.5 g) was added to the filtrate. After the solution had been stirred at room temperature for 1 h, the solution was allowed to stand in a refrigerator overnight. The resulting precipitates were removed by centrifugal separation, and KCl (0.5 g) was added to the filtrate again. After the solution was stirred at room temperature for 1 h, the solution was allowed to stand in a refrigerator overnight. The produced black solid was filtered off. The black solid was washed with ethanol and acetone and finally dried at 70 °C (0.16 g, 39% based on W).

IR (KBr): ν = 1161 (w), 1090 (s), 1018 (m), 950 (s), 905 (s), 811 (s), 773 (vs), 699 (sh) cm^{-1}. UV−vis (0.5 M KH_2PO_4): λ_{max} = 429 nm ($\varepsilon = 2.2 \times 10^3$ dm^3 mol^{-1} cm^{-1}) and 684 nm ($\varepsilon = 1.5 \times 10^3$ dm^3 mol^{-1} cm^{-1}). Cyclic voltammogram: $E_{1/2}$ ($Ru^{IV/III}$) = 1148 mV and $E_{1/2}$ ($Ru^{III/II}$) = 248 mV in 0.5 M KH_2PO_4 aqueous solution (pH 4.3). ^1H NMR (D_2O): (δ/ppm) 3.15 (s) (cf. 4.659 ppm for HOD). ^{13}C NMR (D_2O): (δ/ppm) 44.46 (cf. 30.103 for $(CH_3)_2CO$). ^{31}P NMR (D_2O): (δ/ppm) −8.61, −13.42. ^{183}W NMR (D_2O): (δ/ppm) 104.2, −71.9, −133.1, −168.7, −180.2, −196.0, −202,7, −206.0, −247.1. Anal. Calcd for $K_8[P_2W_{17}O_{61}Ru(C_2H_6SO)]\cdot 16H_2O$: C 0.49; H 0.77; P 1.25; W 63.22; Ru 2.04; K 6.3; Na 0; S 0.65; Cl 0%. Found: C 0.57; H

dx.doi.org/10.1021/ic403041s | Inorg. Chem. 2014, 53, 3526−3539

0.69; P 1.25; W 63.2; Ru 2.15; K 6.47; Na,<0.005; S 0.67; Cl <0.1%. Negative ion MS (CH_3CN-H_2O): calculated for $[P_2W_{17}O_{61}Ru(DMSO)H_2K]^{4-}$ m/z = 1095.9267, found m/z = 1095.9244 (Supporting Information Figure S2).

Preparation of $K_7[P_2W_{17}O_{61}Ru^{III}(H_2O)]$. $Ru_2(benzene)_2Cl_4$ (0.085 g, 0.17 mmol), $K_{10}[\alpha_2\text{-}P_2W_{17}O_{61}]\cdot 15H_2O$ (1.592 g, 0.33 mmol), and water (20 mL) were poured into a 100 mL Teflon-liner autoclave (pH of the solution was 6.0). The autoclave was placed in a conventional oven heated at 170 °C for 5 h. After the autoclave had been cooled to room temperature, the reaction mixture was filtered. Subsequently, 15 mL of acetone was added to the filtrate, and the solution was stirred at room temperature for 1 h. The resulting precipitates were removed by centrifugation, and another 100 mL of acetone was poured into the solution. After the solution had been stirred at room temperature for 30 min, the dark-brown suspension was allowed to stand in a refrigerator overnight. The produced dark-brown solid was filtered off, washed with 100 mL of acetone, and finally dried at 70 °C (0.67 g, 42% based on W).

IR (KBr): ν = 1090 (s), 1080 (s), 1055 (sh), 1014 (m), 949 (s), 914 (s), 817 (sh), 777 (vs), 719 (sh) cm^{-1}. Cyclic voltammogram: $E_{1/2}$ ($Ru^{V/IV}$) = 865 mV, $E_{1/2}$ ($Ru^{IV/III}$) = 516 mV, and $E_{1/2}$ ($Ru^{III/II}$) = −23 mV in 0.5 M KH_2PO_4 aqueous solution (pH 4.3). Negative ion MS (CH_3CN-H_2O): calculated for $[P_2W_{17}O_{61}RuOH_3]^{4-}$ m/z = 1070.9331, found m/z = 1070.9338 (Supporting Information Figure S2). Elemental analysis was performed after conversion to the DMSO derivative (see below).

Preparation of $K_8[\alpha_1\text{-}P_2W_{17}O_{61}Ru^{II}(DMSO)]\cdot 4KCl\cdot 22H_2O$. $K_7[P_2W_{17}O_{61}Ru(H_2O)]$ (0.745 g, 0.43 mmol) and dimethylsulfoxide (DMSO, 1 mL, 14.08 mmol) were dissolved in 49 mL of water, and the solution was stirred at 80 °C using an oil bath for 4 days. After the resulting dark-brown solution had been cooled to room temperature, KCl (1.5 g) was added to the solution, which was stirred to dissolve the KCl and then kept in an open beaker under ambient conditions overnight. The resulting precipitate was filtered off, and KCl (1.5 g) was added to the filtrate again. After the solution had been stirred at room temperature for 1 h, the solution was allowed to stand in a refrigerator overnight. After the resulting precipitate had been filtered off, a deep-green filtrate was obtained. Subsequently, 15 mL of acetone was added to the filtrate, and the solution was stirred at room temperature for 1 h. The resulting precipitate was filtered off, and another 100 mL of acetone was poured into the solution. After the solution had been stirred at room temperature for 30 min, the deep-green suspension was allowed to stand in a refrigerator overnight. The produced black solid was filtered off, washed with 100 mL of acetone, and finally dried at 70 °C (0.59 g, 80% based on W).

IR (KBr): ν = 1158 (w), 1082 (s), 1015 (m), 946 (m), 906 (s), 820 (vs), 781 (vs), 719 (s) cm^{-1}. UV−vis (0.5 M KH_2PO_4): λ_{max} = 445 nm (ε = 1.7 × 10^3 dm^3 mol^{-1} cm^{-1}) and 597 nm (ε = 2.0 × 10^3 dm^3 mol^{-1} cm^{-1}). Cyclic voltammogram: $E_{1/2}$ ($Ru^{IV/III}$) = 1138 mV and $E_{1/2}$ ($Ru^{III/II}$) = 357 mV in 0.5 M KH_2PO_4 aqueous solution (pH 4.3). ^1H NMR (D_2O): (δ/ppm) 3.16 (s, 3*H*), 3.08 (s, 3*H*) (cf. 4.659 for HOD). ^{13}C NMR (D_2O): (δ/ppm) 44.18, 43.02 (cf. 30.103 for $(CH_3)_2CO$). ^{31}P NMR (D_2O): (δ/ppm) −9.67, −12.84. ^{183}W NMR (D_2O): (δ/ppm) 212.4, 127.4, 35.3, −104.4, −122.4, −127.5, −130.1, −137.1, −154.8, −157.2, −159.0, −169.1, −187.3, −200.9, −204.4, −217.7. Anal. Calcd for $K_8[P_2W_{17}O_{61}Ru(C_2H_6SO)]\cdot 4KCl\cdot 22H_2O$: C 0.45; H 0.94; P 1.16; W 58.4; Ru 1.89; K 8.77; Na 0; S 0.60; Cl 2.65%. Found: C 0.67; H 0.71; P 1.21; W 58.3; Ru 2.05; K 8.94; Na,<0.01; S 0.45; Cl 2.54%. Negative ion MS (CH_3CN-H_2O): calculated for $[P_2W_{17}O_{61}Ru(DMSO)H_2K]^{4-}$ m/z = 1095.9267, found m/z = 1095.9247 (Supporting Information Figure S2).

Preparation of Single Crystals for Single-Crystal X-ray Analysis. Crystals suitable for single-crystal X-ray analysis were obtained according to the procedures described below. The identity of the polyanions in crystals was confirmed by CV and ^{31}P NMR.

Single Crystals of $K_8[\alpha_2\text{-}P_2W_{17}O_{61}Ru(DMSO)]$. Crystals suitable for single-crystal X-ray analysis were obtained as a potassium salt by slow diffusion of EtOH−MeOH mixed solvent into an aqueous solution. $K_8[\alpha_2\text{-}P_2W_{17}O_{61}Ru(DMSO)]$ (ca. 0.02 g) was dissolved in water (2 mL), and the solution was filtrated. A vessel containing the filtrate was placed in a closed beaker containing EtOH−MeOH mixed solvent (EtOH, 90 vol %; MeOH, 10 vol %) at room temperature. A few months later, small crystals suitable for single-crystal X-ray analysis were obtained.

Single Crystals of $K_8[\alpha_1\text{-}P_2W_{17}O_{61}Ru(DMSO)]$. Crystals suitable for single-crystal X-ray analysis were obtained as a potassium salt by slow diffusion of acetone into an aqueous solution. $K_8[\alpha_1\text{-}P_2W_{17}O_{61}Ru(DMSO)]$ (ca. 0.02 g) was dissolved in water (2 mL), and the solution was filtrated. A vessel containing the filtrate was placed in a closed beaker containing acetone at room temperature. Several weeks later, small crystals suitable for single-crystal X-ray analysis were obtained. Anal. Calcd for $K_8[P_2W_{17}O_{61}Ru(C_2H_6SO)]\cdot 0.8KCl\cdot 16H_2O$: C 0.48; H 0.77; P 1.24; W 62.5; Ru 2.02; K 6.88; Na 0; S 0.64; Cl 0.57%. Found: C 0.67; H 0.72; P 1.25; W 62.3; Ru 2.16; K 6.66; Na,<0.01; S 0.67; Cl 0.67%.

X-ray Crystallography. *$K_8[\alpha_2\text{-}P_2W_{17}O_{61}Ru(DMSO)]$.* Single-crystal X-ray analysis of $K_8[\alpha_2\text{-}P_2W_{17}O_{61}Ru(DMSO)]$ was performed on a Bruker APEX II single-crystal diffractometer equipped with a Mo Kα anode and graphite monochromator (λ = 0.710 73 Å). The measurement was carried out at 123(2) K. The SHELX software package (Bruker) was used to solve and refine the structure.[23] Absorption corrections were applied empirically using the SADABS program.[24] Carbon atoms and oxygen atoms of water and DMSO molecules were refined isotropically, and other atoms were refined anisotropically. Positions of potassium atoms were determined from a differential Fourier map. The hydrogen atoms of the DMSO ligand were placed geometrically using a riding model. The hydrogen atoms of crystal waters were not located. Although 8 potassium atoms were found in the elemental analysis, only 6.7 potassium atoms were found in the single-crystal structure analysis, due to disorder. Less water was found in the crystal structure than in the elemental analysis, because some of the water molecules were significantly disordered and could not be determined from the differential Fourier map. Crystallographic data are summarized in Table 1.

$K_8[\alpha_1\text{-}P_2W_{17}O_{61}Ru(DMSO)]$. Data collection was performed on a high-precision diffractometer installed in the SPring-8 BL40XU beamline.[25,26] The synchrotron radiation emitted from a helical undulator was monochromated by using an Si(111) channel cut monochromator. A Rigaku Saturn724 CCD detector was used. The

Table 1. Crystal Data and Structure Refinement

	$K_8[\alpha_1\text{-}P_2W_{17}O_{61}Ru(DMSO)]\cdot 16H_2O$	$K_8[\alpha_2\text{-}P_2W_{17}O_{61}Ru(DMSO)]\cdot 16H_2O$
empirical formula	$C_2H_{38}O_{78}SK_8P_2W_{17}Ru$	$C_2H_{38}O_{78}SK_8P_2W_{17}Ru$
M_r	4943.40	4770.96
color and shape	black, plate	black, plate
T/K	100(2)	123(2)
cryst syst	triclinic	monoclinic
space group (No.)	$P\bar{1}$ (2)	$P2_1/m$ (11)
a/Å	12.5844(5)	13.173 (2)
b/Å	15.1035(6)	20.597 (4)
c/Å	22.2140(9)	14.857 (3)
α/deg	97.9960(14)	90
β/deg	90.9513(15)	115.395 (2)
γ/deg	112.9434(12)	90
V/Å^3	3838.7(3)	3641.6 (12)
Z	2	2
R_{int}	0.0496	0.0561
D_c/g cm^{-3}	4.140	4.509
μ/mm^{-1}	38.723	27.580
R_1 [$I > 2\sigma(I)$][a]	0.0883	0.0552
R_w (all data)[b]	0.2679	0.1649

[a] $R_1 = \Sigma||F_o| - |F_c||/\Sigma|F_o|$. [b] $R_w = \{\Sigma w[(F_o^2 - F_c^2)^2]/\Sigma[w(F_o^2)^2]\}^{1/2}$.

dx.doi.org/10.1021/ic403041s | Inorg. Chem. 2014, 53, 3526−3539

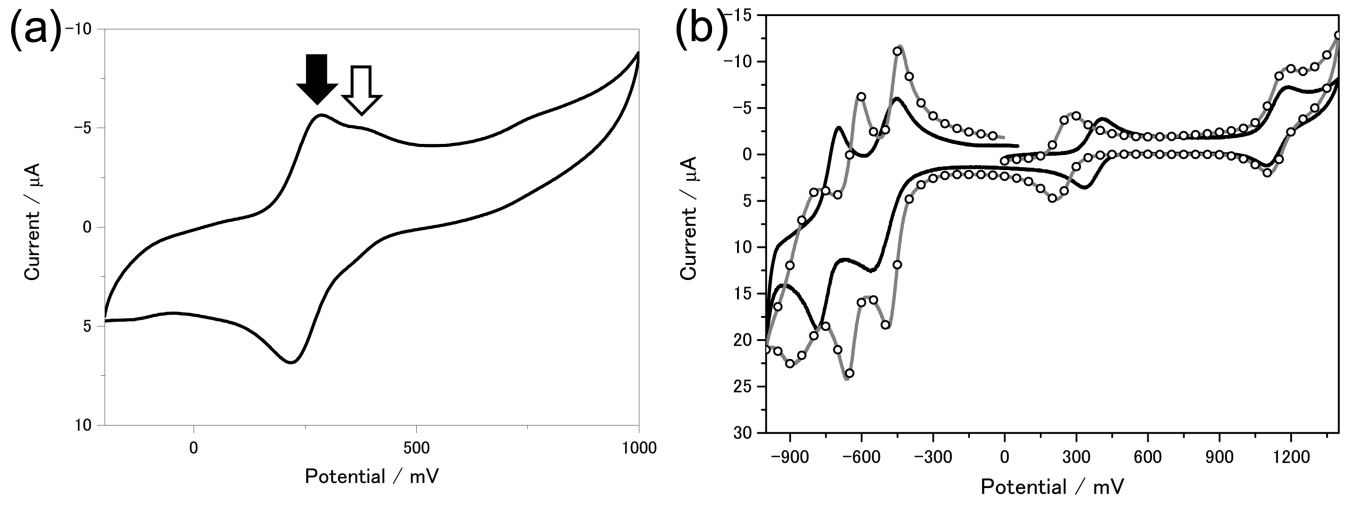

Figure 2. (a) CV of the reaction mixture obtained after reaction of $[\alpha_2\text{-}P_2W_{17}O_{61}]^{10-}$ and $Ru(DMSO)_4Cl_2$ in water at 140 °C for 5 h. The reaction mixture (0.2 mL) was diluted with 0.54 M KH_2PO_4 (2.8 mL) to obtain a solution containing ca. 1.0 mM of Ru and 0.5 M KH_2PO_4 (pH 4.3). The white and black arrows indicate that there are two redox waves. (b) Cyclic voltammograms of isolated black solids (black line) (**D**) $K_8[\alpha_1\text{-}P_2W_{17}O_{61}Ru(DMSO)]$ and (gray line with open circles) (**A**) $K_8[\alpha_2\text{-}P_2W_{17}O_{61}Ru(DMSO)]$ (ca. 1.0 mM in 0.5 M KH_2PO_4 (pH 4.3)).

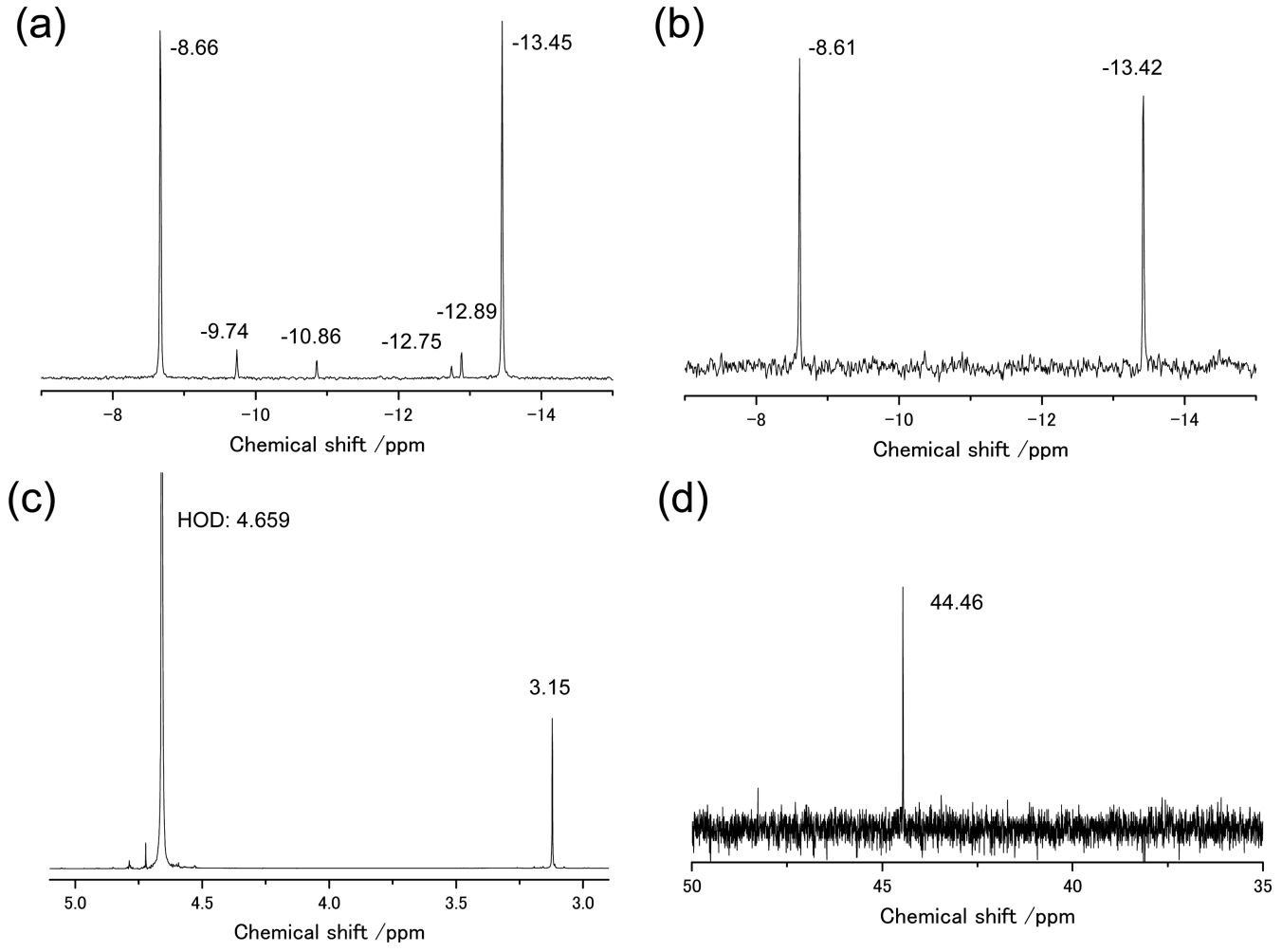

Figure 3. (a) ^{31}P NMR spectrum of the reaction mixture of $[\alpha_2\text{-}P_2W_{17}O_{61}]^{10-}$ and $Ru(DMSO)_4Cl_2$ (ca. 16.6 mM of Ru) in water. The reaction mixture was obtained after reaction at 140 °C for 5 h. Ascorbic acid (ca. 10 equiv) was added. (b) ^{31}P NMR, (c) ^{1}H NMR, and (d) ^{13}C NMR spectra of the isolated black solid **A** ($K_8[\alpha_2\text{-}P_2W_{17}O_{61}Ru(DMSO)]$) in D_2O (ca. 10 mg with 1.0 mL of D_2O).

measurement was performed at 100(2) K. An empirical absorption correction based on Fourier series approximation was applied. The data were corrected for Lorentz and polarization effects. The completeness was slightly low due to the diffractometer which has

dx.doi.org/10.1021/ic403041s | Inorg. Chem. 2014, 53, 3526−3539

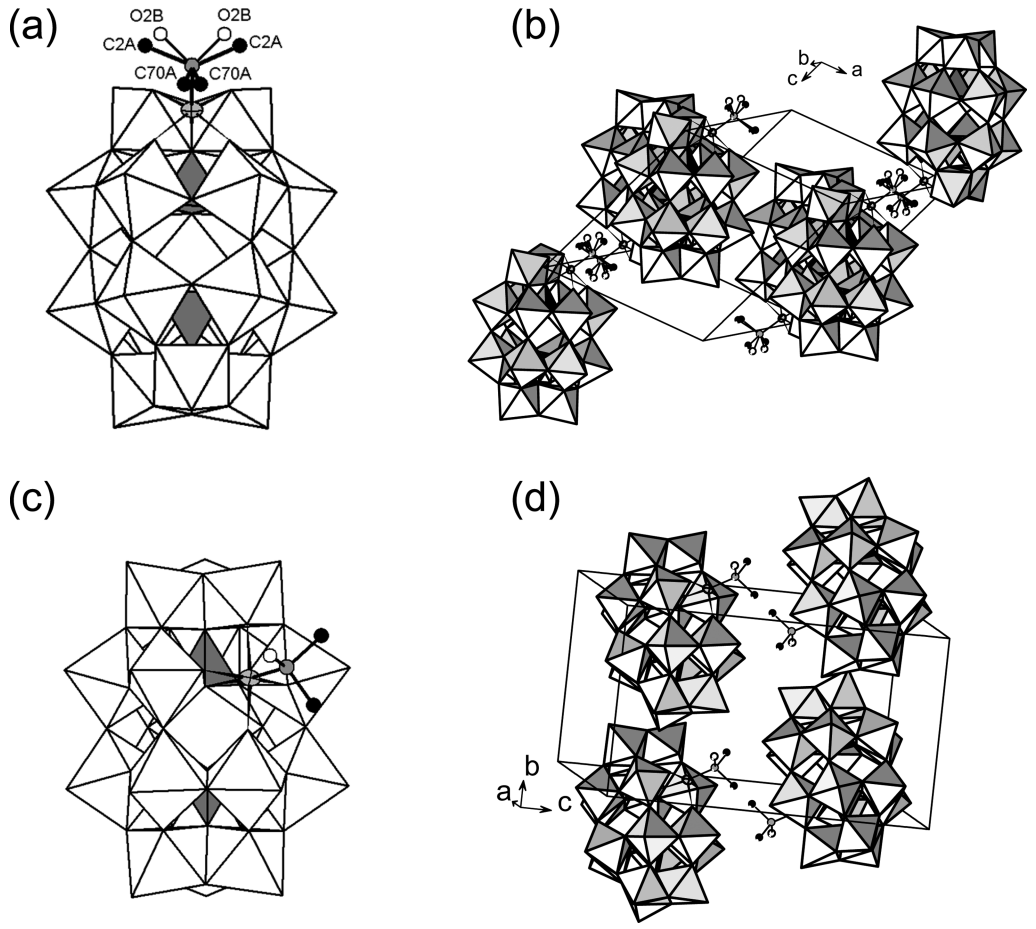

Figure 4. Molecular structures and packings in unit cells of (a and b) $[\alpha_2\text{-}P_2W_{17}O_{61}Ru(DMSO)]^{8-}$, and (c and d) $[\alpha_1\text{-}P_2W_{17}O_{61}Ru(DMSO)]^{8-}$.

only an ω-axis. The structure was solved by direct methods and refined by full-matrix least-squares (SHELX-97),[27] where the unweighted and weighted agreement factors of $R = \Sigma||F_o| - |F_c||/\Sigma|F_o|$ ($I > 2.00\sigma(I)$) and wR = $[\Sigma w(F_o^2 - F_c^2)^2/\Sigma w(F_o^2)^2]^{1/2}$, respectively, were used. Phosphorus atoms, sulfur atoms, and oxygen atoms of water molecules were refined isotropically, and other atoms were refined anisotropically. Positions of potassium atoms and ruthenium atoms were determined from a differential Fourier map. Disorder of Ru and W on four sites, Ru5/W5, Ru10/W10, Ru11/W11, and Ru18/W18, in the belt position was observed (Supporting Information Figure S3). The DMSO molecule was allowed to coordinate to only the Ru18 atom with the highest Ru occupancy of 0.654. The hydrogen atoms of the DMSO molecule were placed geometrically and refined as the riding model. The hydrogen atoms of crystal water were not located. Although 8.8 potassium atoms and 0.8 chloride atoms were found in the elemental analysis, only 5.58 potassium atoms were found in the single-crystal structure analysis, due to disorder. 0.8 KCl was found by elemental analysis, but no Cl was found in the single-crystal structure analysis. We think that KCl was not included in the single-crystal lattice. Less water was found in the crystal structure than in the elemental analysis, because some of the water molecules were significantly disordered and could not be determined from the differential Fourier map. The large residual peaks may be ghost peaks due to the heavy atoms, because structure refinement was unstable and *R*-factor increased for the disordered model including these residual peaks. Crystallographic data are summarized in Table 1.

Further details of the crystal structure investigation may be obtained from the Cambridge Crystallographic Data Centre (CCDC), 12 Union Road, Cambridge CB2 1EZ, U.K. [fax (internat) +44 1223/336-033; e-mail deposit@ccdc.cam.ac.uk], upon quoting the depository numbers CCDC 957156 and 958069, respectively, for $K_8[\alpha_1\text{-}P_2W_{17}O_{61}Ru(DMSO)]$ and $K_8[\alpha_2\text{-}P_2W_{17}O_{61}Ru(DMSO)]$.

Other Analytical Techniques. Infrared (IR) spectra were recorded on a Nicolet 6700 FT-IR spectrometer (Thermo Fisher Scientific) as KBr pellets. Cyclic voltammetry was performed on a CHI620D system (BAS Inc.) at ambient temperature. A glassy carbon working electrode (diameter, 3 mm), a platinum wire counter electrode, and a Ag/AgCl reference electrode (203 mV vs NHE at 25 °C) (3 M NaCl, BAS Inc.) were used. Approximate formal potential values ($E_{1/2}$ values) were calculated from the cyclic voltammograms as the average of cathodic and anodic peak potentials for corresponding oxidation and reduction waves. UV−vis spectra were recorded at ambient temperature using an 8453 UV−vis spectrometer (Agilent) with a 1-cm quartz cell. UV−vis measurements of electrochemically produced species were performed at ambient temperature using an 8453 UV−vis spectrophotometer (Agilent) with a 0.5 mm electrochemical quartz cell (SEC-C, BAS Inc.). The working electrode was an Au-mesh electrode. A platinum wire counter electrode and Ag/AgCl reference electrode (203 mV vs NHE at 25 °C) (3 M NaCl, BAS Inc.) were used. Potential was applied by means of an HAB-151 potentiostat (Hokuto Denko Ltd.). ^{1}H NMR spectra were recorded on a Varian system 500 (500 MHz) spectrometer (Agilent) (H resonance frequency: 499.827 MHz). The spectra were referenced to internal HOD (4.659 ppm) in D_2O. ^{13}C NMR spectra were recorded on a Varian system 500 (500 MHz) spectrometer (Agilent) (C resonance frequency: 125.681 MHz). The spectra were referenced to external $(CH_3)_2CO$ (30.103 ppm). ^{31}P NMR spectra were recorded on a Varian system 500 (500 MHz) spectrometer (Agilent) (P resonance frequency 202.333 MHz). The spectra were referenced to external 85% H_3PO_4 (0 ppm). ^{183}W NMR spectra were recorded on an ECA500 (500 MHz) spectrometer (JEOL) (W resonance frequency 20.839 MHz). The spectrum was referenced to external saturated Na_2WO_4 (0 ppm). The sample of $K_8[\alpha_1\text{-}P_2W_{17}O_{61}Ru(DMSO)]$ for ^{183}W NMR spectroscopy was treated

dx.doi.org/10.1021/ic403041s | *Inorg. Chem.* 2014, 53, 3526−3539

with lithium resin in order to increase solubility in D_2O. Elemental analyses were carried out by Mikroanalytisches Labor Pascher (Remagen, Germany). High-resolution ESI-MS spectra were recorded on a LTQ Orbitrap XL (Thermo Fisher Scientific). A 5 mg portion of each sample was dissolved in 5 mL of H_2O, and these solutions were diluted by CH_3CN (final concentration: ca. 10 μg/mL).

RESULTS AND DISCUSSION

Preparation, Isolation, and Structural Characterization of $K_8[\alpha_2$-$P_2W_{17}O_{61}Ru(DMSO)]$. A monolacunary α_2-Dawson-type phosphotungstate, $[\alpha_2$-$P_2W_{17}O_{61}]^{10-}$, and $Ru(DMSO)_4Cl_2$ (DMSO = dimethyl sulfoxide) are reacted in water at 140 °C for 5 h. Figure 2a shows a cyclic voltammogram (CV) of the reaction mixture diluted in phosphate solution. One large reversible redox pair at ca. 254 mV and a small reversible redox pair at ca. 368 mV are observed and can be assigned to redox potential of Ru in heteropolytungstate. Figure 3a shows the ^{31}P NMR spectrum of the reaction mixture. In order to reduce any Ru^{III} species into Ru^{II} species, ascorbic acid as a reducing reagent is added before NMR measurements.[16] Two large peaks at −8.66 and −13.45 ppm (integration ratio ca. 1: 1) are observed with four small peaks. The small peaks at −10.86 and −12.75 ppm can be assigned to $[PW_{11}O_{39}Ru(DMSO)]^{5-}$ and $[P_2W_{18}O_{62}]^{6-}$, respectively.[9,28] Small peaks at −9.74 and −12.89 ppm with an integration ratio of 1: 1 may correspond to another Dawson-type heteropolytungstate.

By addition of KCl to the reaction mixture, we isolate a black solid (denoted as black solid **A**). As shown in Figure 3b, the ^{31}P NMR spectrum of the isolated black solid **A** in D_2O shows two lines appearing at −8.61 and −13.42 ppm (integration ratio of 1: 1), suggesting the presence of a single species without any phosphorus-containing impurities. Furthermore, the observed ^{31}P NMR chemical shifts are in the usual region for diamagnetic species of various Dawson-type POMs,[29] supporting the presence of diamagnetic Ru^{II}.

Figure 2b shows a CV of the isolated black solid **A** dissolved in 0.5 M KH_2PO_4 (pH 4.3). No trace of other Ru-substituted heteropolytungstates is detected.

These results indicate that a new Ru^{II}-substituted Dawson-type heteropolytungstates is isolated in a pure form.

Single-crystal X-ray structure analysis reveals that the molecular structure of the isolated black solid **A** is composed of a mono-Ru-substituted α_2-Dawson-type phosphotungstate and a DMSO molecule (Figure 4a). The Ru atom is fully incorporated into the α_2-Dawson unit with Ru−O(P) (2.255(16) Å) being shorter than the other 17 W−O(P) bonds (2.340−2.395 Å). The Ru atom is coordinated by five oxygen atoms of the α_2-Dawson unit and by the DMSO molecule through an Ru−S bond (2.046(10) Å). The molecule lies on a crystallographic mirror symmetry that involves W8, Ru, P1, and P2 and make half of the molecule independent. There are two symmetrically related molecules in one unit cell (Figure 4b). The bond valence sum (BVS) values for the 17 W atoms were in the range 6.00−6.30, and the values for the P atom are 4.84 and 5.00, suggesting a formal valence of 6+ for W and 5+ for P, respectively.

As shown in Figure 5a, the IR spectrum of the isolated black solid **A** shows a typical Dawson-type phosphotungstate structure together with a weak peak around 1161 cm^{-1} that is assigned to an S−O stretching vibration peak for the coordinated DMSO ligand.[9,15,16] These data together with results of elemental analysis and high resolution mass

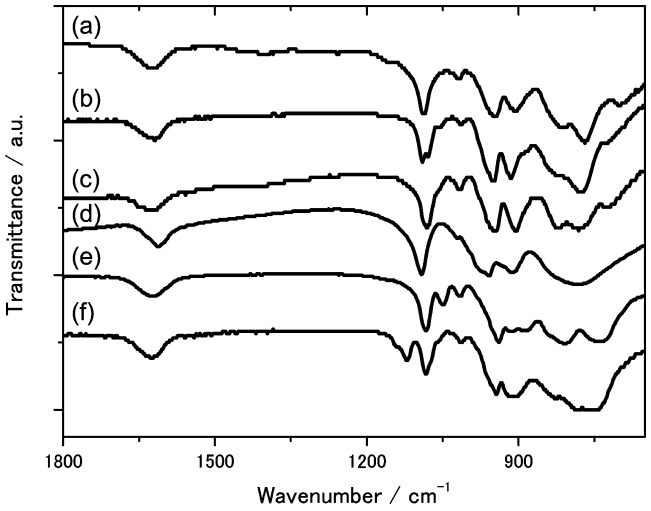

Figure 5. IR spectra of (a) $K_8[\alpha_2$-$P_2W_{17}O_{61}Ru(DMSO)]$ (**A**), (b) $K_7[P_2W_{17}O_{61}Ru(H_2O)]$ (**B**), (c) $K_8[\alpha_1$-$P_2W_{17}O_{61}Ru(DMSO)]$ (**D**), (d) $K_6[P_2W_{18}O_{62}]$, (e) $K_{10}[\alpha_2$-$P_2W_{17}O_{61}]$, and (f) $K_{10}[\alpha_1$-$P_2W_{17}O_{61}]$.

spectroscopy (Supporting Information Figure S2) indicate that the isolated black solid **A** is pure $K_8[\alpha_2$-$P_2W_{17}O_{61}Ru(DMSO)]$.

The ^{183}W NMR spectrum of $K_8[\alpha_2$-$P_2W_{17}O_{61}Ru(DMSO)]$ in D_2O shows nine lines appearing at 104.2, −71.9, −133.1, −168.7, −180.2, −196.0, −202,7, −206.0, and −247.1 with an integration ratio of 2:2:2:2:1:2:2:2:2 (Figure 6a), typical for the

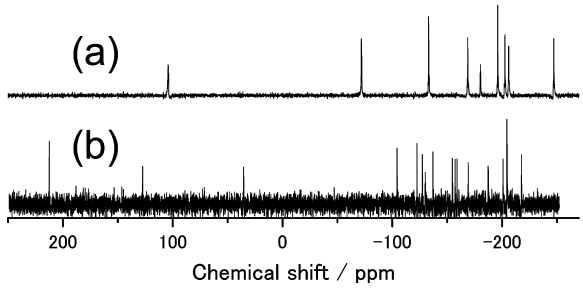

Figure 6. ^{183}W NMR spectra of (a) $[\alpha_2$-$P_2W_{17}O_{61}Ru(DMSO)]^{8-}$ (ca. 0.94 g of $K_8[\alpha_2$-$P_2W_{17}O_{61}Ru(DMSO)]$ with 2.5 mL of D_2O) and (b) $[\alpha_1$-$P_2W_{17}O_{61}Ru(DMSO)]^{8-}$ (ca. 0.25 g of $K_8[\alpha_1$-$P_2W_{17}O_{61}Ru(DMSO)]$ with 2.5 mL of D_2O with help of Li-resin). About 1 equiv of ascorbic acid was added.

α_2-isomer of a monometal-substituted Dawson-type structure with C_s symmetry.[30]

The ^1H NMR spectrum shows one peak appearing at 3.15 ppm that corresponded to the proton of the methyl group of DMSO coordinated to diamagnetic Ru^{II} (Figure 3c).[9,16] This chemical shift is very close to the ^1H NMR chemical shift of $[PW_{11}O_{39}Ru^{II}(DMSO)]^{5-}$ (3.19 ppm) (Table 2) where DMSO is coordinating to Ru through the Ru−S, confirming that DMSO is coordinating to Ru through Ru−S bond in $[\alpha_2$-$P_2W_{17}O_{61}Ru^{II}(DMSO)]^{8-}$. The ^{13}C NMR spectrum also shows one peak appearing at 44.46 ppm that is assignable to the carbon of the methyl group of DMSO (Figure 3d). In the coordinated DMSO ligand, both the carbon atoms and the hydrogen atoms seem to be equivalent because of free rotation on the NMR time scale.[9,15,16,29,31]

dx.doi.org/10.1021/ic403041s | Inorg. Chem. 2014, 53, 3526−3539

Table 2. Comparison of ^{1}H NMR Values and Redox Potentials of Mono-Ru-Substituted Heteropolytungstates with DMSO Ligand

compd	^{1}H NMR[a]/ppm	$Ru^{III/II}$[b]/mV	$Ru^{IV/III}$[b]/mV	ref
$[\alpha_1\text{-}P_2W_{17}O_{61}Ru^{II}(DMSO)]^{8-}$	3.08 3.16	357	1138	this work
$[\alpha_2\text{-}P_2W_{17}O_{61}Ru^{II}(DMSO)]^{8-}$	3.15	248	1148	this work
$[\alpha\text{-}PW_{11}O_{39}Ru^{II}(DMSO)]^{5-}$	3.19	376	1388	16
$[\alpha\text{-}GeW_{11}O_{39}Ru^{II}(DMSO)]^{6-c}$	3.25	238	1218	16
$[\alpha\text{-}SiW_{11}O_{39}Ru^{II}(DMSO)]^{6-c}$	3.21	181	1176	16

[a]Internal standard HOD (4.659 ppm). [b]Reference electrode was Ag/AgCl (3 M NaCl). 0.5 M KH_2PO_4 solution (pH 4.3) was used. [c]Generated by reduction using ascorbic acid (10 equiv) in D_2O.

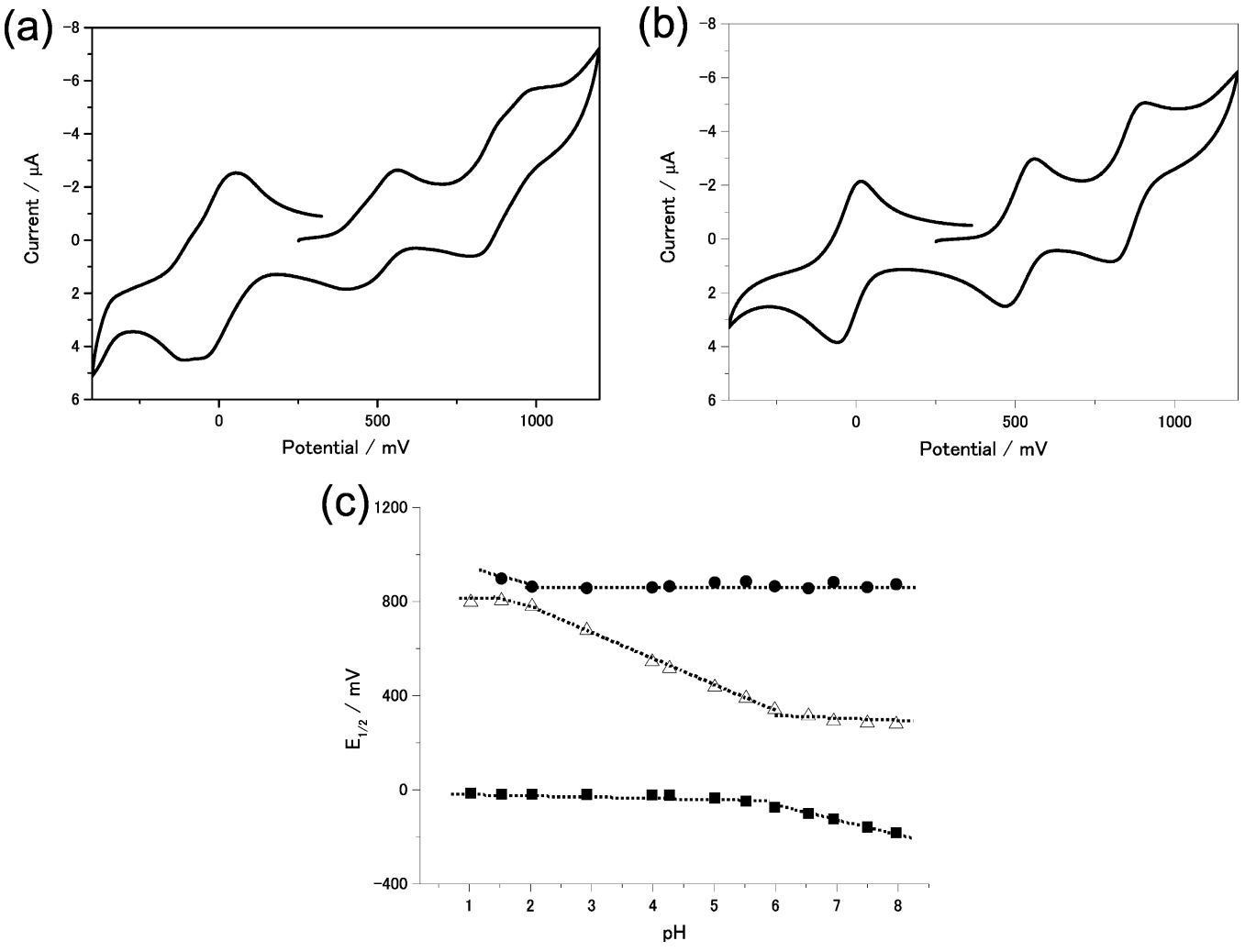

Figure 7. (a) Cyclic voltammogram of the reaction mixture of $[\alpha_2\text{-}P_2W_{17}O_{61}]^{10-}$ and $Ru_2(benzene)_2Cl_4$ (ca. 16.6 mM of Ru) dissolved in 0.5 M KH_2PO_4 (pH 4.3). The reaction mixture (0.1 mL) was diluted with 0.526 M KH_2PO_4 (1.9 mL) to obtain a solution containing ca. 0.85 mM of Ru and 0.5 M KH_2PO_4. The reaction mixture was obtained after reaction at 170 °C for 5 h. (b) Cyclic voltammogram of isolated $K_7[P_2W_{17}O_{61}Ru(H_2O)]$ (**B**) (ca. 10 mg) in 0.5 M KH_2PO_4 (pH 4.3, 3 mL). (c) pH dependence on redox potential $E_{1/2}$ for (●) $Ru^{V/IV}$, (△) $Ru^{IV/III}$, and (■) $Ru^{III/II}$.

These results clearly indicate that the isolated $K_8[\alpha_2\text{-}P_2W_{17}O_{61}Ru(DMSO)]$ is pure and stable in aqueous solution.

Preparation, Isolation, and Structural Characterization of $K_7[P_2W_{17}O_{61}Ru(H_2O)]$. The monolacunary α_2-Dawson-type phosphotungstate $[\alpha_2\text{-}P_2W_{17}O_{61}]^{10-}$ and $Ru_2(benzene)_2Cl_4$ are reacted in water at 170 °C for 5 h. Figure 7a shows a CV of the reaction mixture diluted in phosphate solution. Three major reversible redox pairs at ca. 850, 510, and −30 mV with shoulder peaks are observed.

By addition of acetone to the reaction mixture, we isolate a brown solid (denoted as brown solid **B**. Figure 7b shows a CV of the isolated brown solid **B** dissolved in 0.5 M KH_2PO_4 (pH 4.3). Similar to the previously reported mono-Ru(H_2O)-substituted α-Keggin type heteropolytungstates,[8,12,14] three well-defined reversible redox pairs ($E_{1/2}$ = 865, 516, and −23

dx.doi.org/10.1021/ic403041s | Inorg. Chem. 2014, 53, 3526−3539

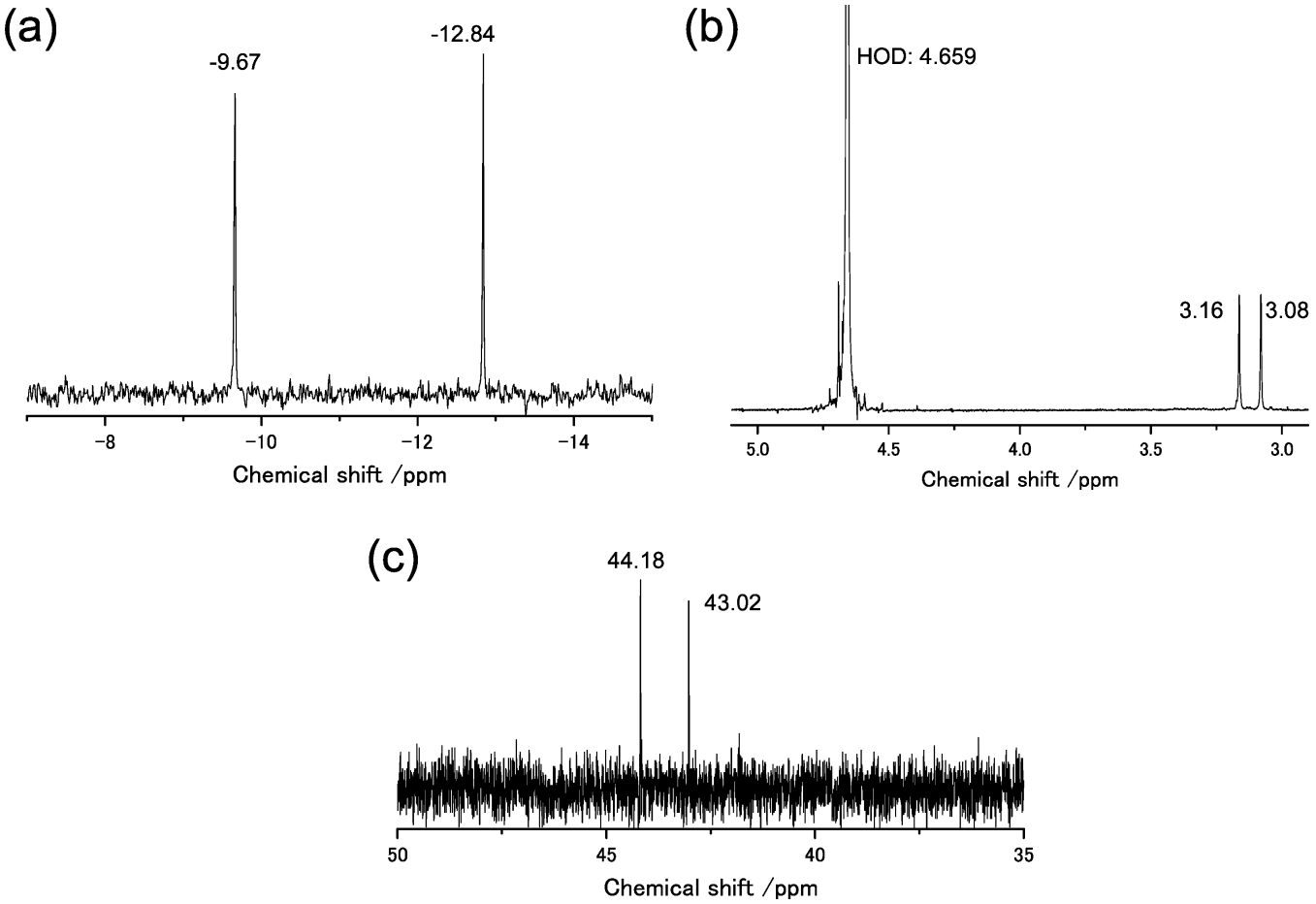

Figure 8. (a) ^{31}P NMR, (b) ^{1}H NMR, and (c) ^{13}C NMR spectra of the isolated K-black solid **D** $K_8[\alpha_1\text{-}P_2W_{17}O_{61}Ru^{II}(DMSO)]$ in D_2O (ca. 10 mg in 1.0 mL of D_2O).

mV) are observed. The peak separations of the redox pairs are typically 70−90 mV, indicating that these electrode processes are reversible one-electron transfers.[32]

The IR spectrum of the isolated brown solid **B** is similar to that of $[P_2W_{18}O_{62}]^{6-}$, indicating that the isolated brown solid **B** is a Ru-substituted Dawson-type phosphotungstate (Figure 5b−d).

Figure 7c shows pH dependence on redox potentials (Pourbaix diagram) of the isolated brown solid **B**. The pH dependencies on three redox potentials are similar to those of the previously reported mono-$Ru(H_2O)$-substituted α-Keggin-type heteropolytungstates,[8] indicating that the isolated brown solid **B** contains monosubstituted $Ru^{III}(H_2O)$ species. This redox behavior together with IR results and high resolution mass spectroscopy (Supporting Information Figure S2) indicate that the isolated brown solid **B** is mono-Ru-substituted Dawson-type heteropolytungstate with an H_2O ligand, $[P_2W_{17}O_{61}Ru^{III}(H_2O)]^{7-}$.

The UV−vis spectrum after electrochemical one-electron reduction at −250 mV (peak max: 457 and 707 nm) (Supporting Information Figure S4) is similar to that of $[XW_{11}O_{39}Ru^{II}(H_2O)]^{n-}$ (X = P and Si).[12,14] This also confirms that the redox pair at −23 mV is a reversible one-electron transfer for $Ru^{III/II}(H_2O)$.

Reaction of $[P_2W_{17}O_{61}Ru^{III}(H_2O)]^{7-}$ with Dimethyl Sulfoxide to Form $[P_2W_{17}O_{61}Ru^{III}(DMSO)]^{7-}$ and Their Structural Characterization. In order to confirm the structure of the prepared $[P_2W_{17}O_{61}Ru^{III}(H_2O)]^{7-}$, we perform transformation of the isolated $[P_2W_{17}O_{61}Ru^{III}(H_2O)]^{7-}$ to the corresponding DMSO-coordinated compound, $[P_2W_{17}O_{61}Ru\text{-}(DMSO)]^{n-}$, for the following two reasons: (1) We can compare CV and NMR spectra with those of isolated $[\alpha_2\text{-}P_2W_{17}O_{61}Ru^{II}(DMSO)]^{8-}$. (2) We have succeeded in confirming an α-Keggin structure of a mono-$Ru(H_2O)$-substituted heteropolytungstates, $[XW_{11}O_{39}Ru^{III}(H_2O)]^{5-}$ (X = Si or Ge), by transformation of the aqua complex to a DMSO-coordinated complex, $[XW_{11}O_{39}Ru^{III}(DMSO)]^{5-}$.[15,16] The DMSO ligand hinders rotation of the molecule in the crystal, and α-Keggin structure and an Ru position can be revealed by single-crystal structure analysis without disorder. Disorder is often observed in the crystals of mono-metal-substituted Keggin-type heteropolytungstates, and substituted metal can not be distinguished from other tungstens.[15] We expect that single-crystal structure analysis of the DMSO-coordinated compound is possible.

Supporting Information Figure S5 shows CVs of the reaction solutions obtained by reaction of $[P_2W_{17}O_{61}Ru^{III}(H_2O)]^{7-}$ with DMSO at 80 °C. Redox pairs corresponding to redox of $[P_2W_{17}O_{61}Ru^{III}(H_2O)]^{7-}$ disappears, and a new redox pair appears. This result indicates that the aqua ligand is substituted by the DMSO ligand. There are three redox couples, large redox couples at ca. −508 and −743 mV and a small one at ca. −632 mV. The small one corresponds to redox of $[\alpha_2\text{-}P_2W_{17}O_{61}Ru^{III/II}(DMSO)]^{n-}$. Addition of CsCl precipitates a black solid (denoted as Cs-black solid **C**), and the CV of the Cs-black solid **C** (Supporting Information Figure S5b) is the same as the CV after the reaction, indicating that the Cs-black

dx.doi.org/10.1021/ic403041s | Inorg. Chem. 2014, 53, 3526−3539

solid **C** is a mixture of $[\alpha_2\text{-}P_2W_{17}O_{61}Ru(DMSO)]^{n-}$ and new Ru(DMSO) species.

Supporting Information Figure S6 shows ^{31}P NMR and ^{1}H NMR spectra of the Cs-black solid **C** in D_2O. Since Ru in the Cs-black solid contains Ru^{III} species, NMR measurement is performed after adding ascorbic acid as a reducing reagent.[16] The ^{31}P NMR spectrum of the Cs-black solid **C** shows four peaks appearing at −8.59, −9.72, −12.80, and −13.30 ppm (integration ratio of ca. 1:7:7:1). The two small peaks at −8.59 and −13.30 ppm are assigned to two peaks of $[\alpha_2\text{-}P_2W_{17}O_{61}Ru^{II}(DMSO)]^{8-}$, and another two large peaks with a 1:1 integration ratio are assignable to another Dawson compound. The ^{1}H NMR spectrum of the Cs-black solid **C** shows a small peak and two large peaks corresponding to the proton of the DMSO ligand coordinated to Ru^{II}. The small peak at 3.15 ppm is assignable to the proton of the DMSO ligand in $[\alpha_2\text{-}P_2W_{17}O_{61}Ru^{II}(DMSO)]^{8-}$ (Supporting Information Figure S6). These results indicate that the Cs-black solid **C** contains an Ru(DMSO)-substituted α_2-Dawson-type phosphotungstate, $[\alpha_2\text{-}P_2W_{17}O_{61}Ru(DMSO)]^{n-}$, as a minor component and its isomer as a major component.

By careful addition of KCl and acetone to the reaction solution obtained by reaction of $[P_2W_{17}O_{61}Ru^{III}(H_2O)]^{7-}$ with DMSO at 80 °C for 4 days, we obtain a black solid (denoted as K-black solid **D**). As shown in Figures 2b and 8a, no trace of $[\alpha_2\text{-}P_2W_{17}O_{61}Ru(DMSO)]^{8-}$ is detected by a CV and ^{31}P NMR technique, indicating that the new compound is isolated in a pure form. Interestingly, a sharp ^{31}P NMR signal is observed without addition of ascorbic acid, indicating that valence of Ru is 2+. DMSO in the reaction mixture acts as a reducing reagent and produces Ru^{II} species. After addition of KCl, the dark brown color of the reaction mixture, typical for an Ru^{III}(DMSO)-substituted heteropolytungstate, changes to dark green, typical for an Ru^{II}(DMSO)-substituted heteropolytungstate. We propose that the presence of potassium cation is favorable for the reduction, because the reduced form has a higher negative charge. Similar behavior was reported for the reduction of $[PMo_{12}O_{40}]^{3-}$, $[SiW_{11}O_{39}Fe^{III}(H_2O)]^{5-}$, and $[SiW_{11}O_{39}Mn^{III}(H_2O)]^{5-}$.[33−35] Increase in the countercation amount is favorable for reduction. In the case of CsCl, we obtain a mixture of Ru^{III}(DMSO) and Ru^{II}(DMSO) species. We think that precipitation with Cs cation is so fast that the Ru^{III}(DMSO) compound is precipitated before reduction to Ru^{II}(DMSO).

Single-crystal X-ray structure analysis reveals that the molecular structure of the K-black solid **D** is composed of a mono-Ru-substituted α_1-Dawson-type phosphotungstate unit and a DMSO molecule (Figure 4c). The Ru atom is coordinated by five oxygen atoms of the α_1-Dawson unit and by the DMSO molecule through an Ru−S bond.

As shown in Figure 5c, the IR spectrum of the isolated K-black solid **D** shows a typical Dawson-type phosphotungstate structure together with a weak peak around 1158 cm^{-1} that is assigned to an S−O stretching vibration peak for the coordinated DMSO ligand.[9,15,16] Although the IR spectrum of $[\alpha_1\text{-}P_2W_{17}O_{61}Ru(DMSO)]^{8-}$ is similar to that of $[\alpha_2\text{-}P_2W_{17}O_{61}Ru(DMSO)]^{8-}$, the W−O stretching vibration peak at 650−850 cm^{-1} is slightly different. It has been reported that IR spectra of α_1- and α_2-isomers of mono-iron-substituted Dawson-type heteropolytungstates are similar.[36] These results together with results of elemental analysis and high resolution mass spectroscopy (Supporting Information Figure S2) indicate that the obtained K-black solid **D** is $K_8[\alpha_1\text{-}P_2W_{17}O_{61}Ru^{II}(DMSO)]$.

As shown in Figure 8a, the ^{31}P NMR spectrum of $K_8[\alpha_1\text{-}P_2W_{17}O_{61}Ru(DMSO)]$ in D_2O shows two lines appearing at −9.67 and −12.84 ppm (integration ratio of 1: 1), which are different from those of $K_8[\alpha_2\text{-}P_2W_{17}O_{61}Ru^{II}(DMSO)]$ at −8.61 and −13.42 ppm. The two clean ^{31}P NMR signals of $K_8[\alpha_1\text{-}P_2W_{17}O_{61}Ru^{II}(DMSO)]$ suggest the presence of a single species without any phosphorus-containing impurities. Furthermore, the observed ^{31}P NMR chemical shifts are in the usual region for diamagnetic species of various Dawson-type POMs,[29] supporting the presence of a diamagnetic Ru^{II} complex.

The ^{183}W NMR spectrum of $[\alpha_1\text{-}P_2W_{17}O_{61}Ru(DMSO)]^{8-}$ in D_2O shows 16 lines appearing at 212.4, 127.4, 35.3, −104.4, −122.4, −127.5, −130.1, −137.1, −154.8, −157.2, −159.0, −169.1, −187.3, −200.9, −204.4, and −217.7 with an integration ratio of 1:1:1:1:1:1:1:1:1:1:1:1:1:1:2:1 (Figure 6b). Integration of the peak at −204.4 ppm is ca. twice of those of other peaks, indicating that two peaks are overlapping. All 17 peaks are observed, being consistent with the unsymmetrical chiral anion $[\alpha_1\text{-}P_2W_{17}O_{61}Ru^{II}(DMSO)]^{8-}$.[17]

Unlike the case of $K_8[\alpha_2\text{-}P_2W_{17}O_{61}Ru^{II}(DMSO)]$, the ^{1}H NMR spectrum of $K_8[\alpha_1\text{-}P_2W_{17}O_{61}Ru(DMSO)]$ shows two peaks appearing at 3.16 and 3.08 ppm (integration ratio of 1: 1) corresponding to two nonequivalent methyl group of DMSO coordinated to diamagnetic Ru^{II} (Figure 8b). The chemical shifts are close to ^{1}H NMR chemical shifts of $[\alpha_2\text{-}P_2W_{17}O_{61}Ru^{II}(DMSO)]^{8-}$ and $[\alpha\text{-}PW_{11}O_{39}Ru^{II}(DMSO)]^{5-}$ (Table 2), indicating that DMSO is coordinating to Ru through Ru−S bond. The ^{13}C NMR spectrum also shows two peaks appearing at 44.18 and 43.02 ppm that are assignable to two nonequivalent carbons of the methyl group of DMSO (Figure 8c). The presence of two ^{1}H NMR and ^{13}C NMR peaks confirms that the two methyl groups of DMSO coordinated to the chiral $\alpha_1\text{-}P_2W_{17}O_{61}Ru$ unit are in a diastereotopic relationship.[37]

These results clearly indicate that the isolated K-black solid **D** is potassium salt of the α_1-isomer of a mono-Ru-substituted Dawson-type phosphotungstate, $K_8[\alpha_1\text{-}P_2W_{17}O_{61}Ru^{II}(DMSO)]$, and this complex is stable in aqueous solution. This is the first report on the preparation and characterization of the α_1-isomer of a mono-Ru-substituted Dawson-type heteropolytungstate.

Reaction of $[\alpha_2\text{-}P_2W_{17}O_{61}]^{10-}$ with $Ru(DMSO)_4Cl_2$ or $Ru_2(benzene)_2Cl_4$. An isomer detected by ^{31}P NMR at −9.74 and −12.89 ppm with a 1:1 integration ratio (Figure 3a) in a reaction solution obtained after reaction of $[\alpha_2\text{-}P_2W_{17}O_{61}]^{10-}$ and $Ru(DMSO)_4Cl_2$ at 140 °C is assigned to $[\alpha_1\text{-}P_2W_{17}O_{61}Ru^{II}(DMSO)]^{8-}$. Reaction of $[\alpha_2\text{-}P_2W_{17}O_{61}]^{10-}$ and $Ru(DMSO)_4Cl_2$ at 140 °C produces $[\alpha_2\text{-}P_2W_{17}O_{61}Ru^{II}(DMSO)]^{8-}$ as the main product and $[\alpha_1\text{-}P_2W_{17}O_{61}Ru^{II}(DMSO)]^{8-}$, $[PW_{11}O_{39}Ru(DMSO)]^{5-}$, and $[P_2W_{18}O_{62}]^{6-}$ as side products (eq 4).

$$\begin{aligned}[\alpha_2\text{-}P_2W_{17}O_{61}]^{10-} + Ru(DMSO)_4Cl_2 \\ \rightarrow [\alpha_2\text{-}P_2W_{17}O_{61}Ru(DMSO)]^{8-}\ (\text{the main product}) \\ + [\alpha_1\text{-}P_2W_{17}O_{61}Ru(DMSO)]^{8-} \\ + [PW_{11}O_{39}Ru(DMSO)]^{5-} + [P_2W_{18}O_{62}]^{6-} \end{aligned} \quad (4)$$

Effect of reaction temperature and reaction time on the yields of Ru-substituted phosphotungstates and their ratios are summarized in Table 3. Temperature higher than 125 °C is

dx.doi.org/10.1021/ic403041s | Inorg. Chem. 2014, 53, 3526−3539

Table 3. Product Yields under Different Conditions

				product ratio[b]		
entry	T/°C	time/h	yield of Ru complexes[a]/%	$[\alpha_1\text{-}P_2W_{17}O_{61}Ru(DMSO)]^{8-}$	$[\alpha_2\text{-}P_2W_{17}O_{61}Ru(DMSO)]^{8-}$	$[\alpha\text{-}PW_{11}O_{39}Ru(DMSO)]^{5-}$
Reaction of $[\alpha_2\text{-}P_2W_{17}O_{61}]^{10-}$ + $Ru(DMSO)_4Cl_2$ → [c]						
1	r.t.	5	n.d.[d]			
2	100	5	n.d.[d]			
3	100	24	28	13	85	<1
4	100	48	49	9	90	<1
5	100	72	60	9	90	1
6	125	5	63	10	86	4
7	140	5	65	6	93	1
8	170	5	95	6	91	3
9	215	5	n.d.[d]			
Reaction of $[\alpha_1\text{-}P_2W_{17}O_{61}]^{10-}$ + $Ru(DMSO)_4Cl_2$ → [c]						
10	140	5	78	43	56	<1
Reaction of $[\alpha_2\text{-}P_2W_{17}O_{61}]^{10-}$ + $Ru_2(benzene)_2Cl_4$, Then the Reaction Mixture Was Reacted with DMSO → [e]						
11	80	5	n.d.[d]			
12	100	5	n.d.[d]			
13	125	5	35	65	17	19
14	140	5	41	78	12	10
15	170	5	66	79	11	10
Reaction of $[\alpha_1\text{-}P_2W_{17}O_{61}]^{10-}$ + $Ru_2(benzene)_2Cl_4$, Then the Reaction Mixture Was Reacted with DMSO → [e]						
16	170	5	20	72	13	14

[a]Yields were estimated by CV after the solution had been mixed with KH_2PO_4 solution (concentrations of Ru and KH_2PO_4 being ca. 1 mM and 0.5 M, respectively). Oxidation peak current of $Ru^{III/II}(DMSO)$ was compared with peak current of authentic $[\alpha_2\text{-}P_2W_{17}O_{61}Ru(DMSO)]^{n-}$ and $[\alpha_1\text{-}P_2W_{17}O_{61}Ru(DMSO)]^{n-}$ to estimate yields in entries 1−10 and 11−16, respectively, although redox waves of $[\alpha_2\text{-}P_2W_{17}O_{61}Ru^{III/II}(DMSO)]^{n-}$, $[\alpha_1\text{-}P_2W_{17}O_{61}Ru^{III/II}(DMSO)]^{n-}$, and $[\alpha\text{-}PW_{11}O_{39}Ru^{III/II}(DMSO)]^{n-}$ were overlapping. [b]Molar ratio was estimated by integration ratio of ^{31}P NMR. Ascorbic acid (ca. 10 equiv to Ru) was added. [c]$[\alpha_1\text{-}/\alpha_2\text{-}P_2W_{17}O_{61}]^{10-}$ (0.156 g, 0.03 mmol) and $Ru(DMSO)_4Cl_2$ (0.016 g, 0.03 mmol) were reacted in D_2O (2 mL). [d]Not dectected. [e]$[\alpha_1\text{-}/\alpha_2\text{-}P_2W_{17}O_{61}]^{10-}$ (0.815 g, 0.17 mmol) and $Ru_2(benzene)_2Cl_4$ (0.04 g, 0.085 mmol) were reacted in H_2O (10 mL). The obtained reaction mixture (9.0 mL) was mixed with DMSO (1.0 mL) and heated at 80 °C for 4 days.

needed to produce the desired substituted compound with a reaction time of 5 h (entries 1, 2, and 6). At the reaction temperature of 100 °C, longer reaction time is needed (entries 2−5). When the temperature is increased up to 170 °C, yields of the Ru-substituted phosphotungstate are increased (entries 6−8). On the other hand, at the reaction temperature of 215 °C, no Ru-substituted product is observed (entry 9). A similar tendency was observed for the production of $[\alpha\text{-}PW_{11}O_{39}Ru^{II}(DMSO)]^{5-}$ from $[\alpha\text{-}PW_{11}O_{39}]^{7-}$ and $Ru(DMSO)_4Cl_2$.[9] $[\alpha\text{-}P_2W_{18}O_{62}]^{6-}$ is always obtained as a side product. Pope's group reported the formation of $[P_2W_{18}O_{62}]^{6-}$ as a byproduct in the preparation of $[P_2W_{17}O_{61}Ru(H_2O)]^{7-}$ by a reaction of $[\alpha_2\text{-}P_2W_{17}O_{61}]^{10-}$ with $[Ru(H_2O)_6](C_7H_7SO_3)_2$.[12] Proust's group also reported the formation of $[P_2W_{18}O_{62}]^{6-}$ as a byproduct in the preparation of $[\alpha_2\text{-}P_2W_{17}O_{61}OsN]^{7-}$ by a reaction of $[\alpha_2\text{-}P_2W_{17}O_{61}]^{10-}$ with $[OsNCl_4]$.[38] The formation of $[\alpha\text{-}PW_{11}O_{39}Ru^{II}(DMSO)]^{5-}$ from $[\alpha_2\text{-}P_2W_{17}O_{61}]^{10-}$ and $Ru(DMSO)_4Cl_2$ indicates decomposition of Dawson-type lacunary compound $[\alpha_2\text{-}P_2W_{17}O_{61}]^{10-}$ to Keggin-type lacunary compound $[\alpha\text{-}PW_{11}O_{39}]^{7-}$, which may include decomposition of $[\alpha_2\text{-}P_2W_{17}O_{61}]^{10-}$ to $[PW_9O_{34}]^{9-}$ followed by a reaction of $[PW_9O_{34}]^{9-}$ with two $[WO_4]^{2-}$ to form $[\alpha\text{-}PW_{11}O_{39}]^{7-}$. Production of $[P_2W_{18}O_{62}]^{6-}$ and $[\alpha\text{-}PW_{11}O_{39}]^{7-}$ by heating of $[\alpha_2\text{-}P_2W_{17}O_{61}]^{10-}$ at 140 and 170 °C without Ru sources is confirmed by ^{31}P NMR (Supporting Information Figure S1d,e). The ratio of Ru-substituted phosphotungstates, $[\alpha_1\text{-}P_2W_{17}O_{61}Ru^{II}(DMSO)]^{8-}$, $[\alpha_2\text{-}P_2W_{17}O_{61}Ru^{II}(DMSO)]^{8-}$, and $[PW_{11}O_{39}Ru(DMSO)]^{5-}$, is also almost same even though yields of Ru-substituted compounds are changed. However, the ratio of $[\alpha_1\text{-}P_2W_{17}O_{61}Ru^{II}(DMSO)]^{8-}$ increases when we use $[\alpha_1\text{-}P_2W_{17}O_{61}]^{10-}$ as a starting compound (entry 10).

The effect of temperature on the Ru-substituted phosphotungstate from $[\alpha_2\text{-}P_2W_{17}O_{61}]^{10-}$ and $Ru_2(benzene)_2Cl_4$ is investigated (Supporting Information Figure S7). At the reaction temperatures of 80 and 100 °C, the starting compound, $[\alpha_2\text{-}P_2W_{17}O_{61}]^{10-}$, and $[\alpha\text{-}P_2W_{18}O_{62}]^{6-}$ are detected. Yields of Ru-substituted phosphotungstates and their formation ratio are analyzed after transformation of their aqua species to DMSO-coordinating species (Table 3). Similar to the case of the reaction between $[\alpha_2\text{-}P_2W_{17}O_{61}]^{10-}$ and $Ru(DMSO)_4Cl_2$, a reaction temperature of more than 125 °C is needed to produce the desired Ru-substituted compound with a reaction time of 5 h.

After reaction of $[P_2W_{17}O_{61}Ru^{III}(H_2O)]^{7-}$ with DMSO, $[\alpha_1\text{-}P_2W_{17}O_{61}Ru^{III}(DMSO)]^{7-}$ is produced as the main product with $[\alpha_2\text{-}P_2W_{17}O_{61}Ru^{III}(DMSO)]^{7-}$ and $[PW_{11}O_{39}Ru^{III}(DMSO)]^{4-}$ as side products (entries 13−15).

Assuming that isomerization does not occur during the reaction of $[P_2W_{17}O_{61}Ru^{III}(H_2O)]^{7-}$ with the DMSO, reaction of $[\alpha_2\text{-}P_2W_{17}O_{61}]^{10-}$ and $Ru_2(benzene)_2Cl_4$ produced $[\alpha_1\text{-}P_2W_{17}O_{61}Ru^{III}(H_2O)]^{7-}$ as the main product and $[\alpha_2\text{-}P_2W_{17}O_{61}Ru^{III}(H_2O)]^{7-}$, $[PW_{11}O_{39}Ru^{III}(H_2O)]^{4-}$, and $[P_2W_{18}O_{62}]^{6-}$ as side products (eq 5).

$$[\alpha_2\text{-}P_2W_{17}O_{61}]^{10-} + \frac{1}{2}Ru_2(benzene)_2Cl_4 \rightarrow [a_1\text{-}P_2W_{17}O_{61}Ru^{III}(H_2O)]^{7-}\ (\text{the main product}) + [\alpha_2\text{-}P_2W_{17}O_{61}Ru^{III}(H_2O)]^{7-} + [PW_{11}O_{39}Ru^{III}(H_2O)]^{4-} + [P_2W_{18}O_{62}]^{6-} \quad (5)$$

dx.doi.org/10.1021/ic403041s | Inorg. Chem. 2014, 53, 3526−3539

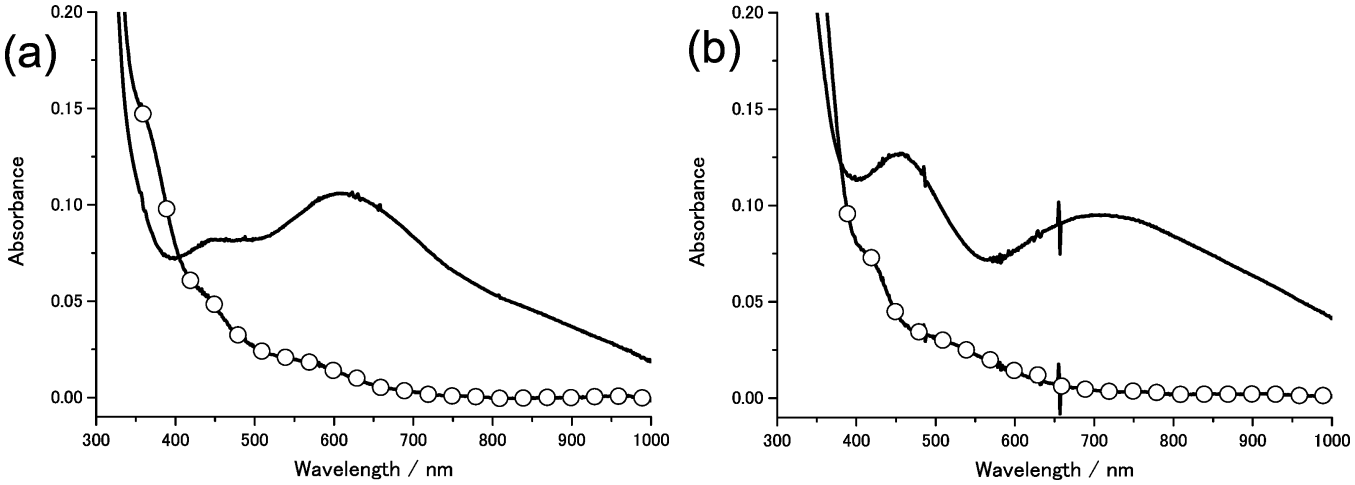

Figure 9. UV−vis spectra of (a) $[\alpha_1\text{-}P_2W_{17}O_{61}Ru(DMSO)]^{n-}$ and (b) $[\alpha_2\text{-}P_2W_{17}O_{61}Ru(DMSO)]^{n-}$ in 0.5 M KH_2PO_4 (pH 4.3). (Solid line) $Ru^{II}(DMSO)$ species and (solid line with open circles) $Ru^{III}(DMSO)$ species generated by electrolysis. Concentration was ca. 1 mM, and cell length was 0.5 mm.

Absence of $[\alpha_1\text{-}P_2W_{17}O_{61}]^{10-}$ in the starting compound, $[\alpha_2\text{-}P_2W_{17}O_{61}]^{10-}$, is confirmed by ^{31}P NMR (Supporting Information Figure S1a−c). These results indicate that the Ru-substituted α_1-isomer, $[\alpha_1\text{-}P_2W_{17}O_{61}Ru(L)]^{n-}$ (L: H_2O or DMSO), is formed from $[\alpha_2\text{-}P_2W_{17}O_{61}]^{10-}$ by isomerization from α_2- isomer to α_1-isomer.

Pope's group reported the synthesis of $[P_2W_{17}O_{61}Ru^{II}(DMSO)]^{8-}$ by electrochemical reduction of $[P_2W_{17}O_{61}Ru^{III}(H_2O)]^{7-}$ to $[P_2W_{17}O_{61}Ru^{II}(H_2O)]^{8-}$ and subsequent reaction with DMSO.[12] They reported ^{31}P NMR signals of their $[P_2W_{17}O_{61}Ru^{II}(DMSO)]^{8-}$ appearing at −8.7 and −13.5 ppm, which are very close to our ^{31}P NMR chemical shifts of $[\alpha_2\text{-}P_2W_{17}O_{61}Ru^{II}(DMSO)]^{8-}$, indicating that their $[P_2W_{17}O_{61}Ru^{II}(DMSO)]^{8-}$ compound is an α_2-isomer. Assuming that isomerization does not occur in the reaction with DMSO, $[P_2W_{17}O_{61}Ru^{III}(H_2O)]^{7-}$ obtained by their method is an α_2-isomer.

There have been some reports about $Ru^{II}(DMSO)_3(H_2O)$ or $Ru^{II}(benzene)(H_2O)$-supported heteropolytungstates in which $Ru^{II}(DMSO)_3(H_2O)$ or $Ru^{II}(benzene)(H_2O)$ is attached on the monolacunary heteropolytungstate.[29,31,39−42] In these compounds, $Ru^{II}(DMSO)_3(H_2O)$ and $Ru^{II}(benzene)(H_2O)$ are coordinated by two oxygen atoms in the vacant site. Proust's group and we have reported that $Ru^{II}(benzene)$-supported Keggin-type heteropolytungstates were intermediates to produce Ru-substituted heteropolytungstates.[8,42] Kortz's group reported preparation of β_3-isomers of $Ru^{II}(DMSO)_3(H_2O)$-supported Keggin-type heteropolytungstates, $[\beta_3\text{-}XW_{11}O_{39}Ru^{II}(DMSO)_3(H_2O)]^{6-}$ (X = Ge and Si).[39] Recently, we reported that reactions of $[\alpha\text{-}XW_{11}O_{39}]^{8-}$ (X = Ge and Si) with $Ru^{II}(DMSO)_4Cl_2$ produced β_3-isomers of $Ru^{II}(DMSO)_3(H_2O)$-supported Keggin-type heteropolytungstates, $[\beta_3\text{-}XW_{11}O_{39}Ru^{II}(DMSO)_3(H_2O)]^{6-}$ at ca. 70 °C, and then Ru(DMSO)-substituted heteropolytungstates, $[\beta_3\text{-}XW_{11}O_{39}Ru^{II}(DMSO)]^{6-}$ (X = Ge and Si) at 125 °C.[43] In the case of Ru-supported and substituted Keggin-type heteropolytungstates, superior stability of the β_3-isomer over the corresponding α-isomer was reported.[40] We propose that the α_1-isomer might be produced in the first reaction step to form an Ru-supported Dawson-type heteropolytungstate. Further investigation about the isomerization will include preparation and structural characterization of $Ru^{II}(DMSO)_3L$ or $Ru^{II}(benzene)L$-supported (L: ligand) Dawson-type heteropolytungstates, and theoretical calculations about the isomerization process are being planned.

Redox Behavior of $[\alpha_1/\alpha_2\text{-}P_2W_{17}O_{61}Ru(DMSO)]^{n-}$. Figure 2b shows cyclic voltammograms of the $K_8[\alpha_1\text{-}P_2W_{17}O_{61}Ru^{II}(DMSO)]$ and $K_8[\alpha_2\text{-}P_2W_{17}O_{61}Ru^{II}(DMSO)]$ dissolved in 0.5 M KH_2PO_4 (pH 4.3). In both cases, two small well-defined reversible redox pairs around 300 and 1150 mV and two large well-defined reversible redox pairs between −300 and −800 mV are observed, similar to those of the previously reported Ru(DMSO)-substituted Keggin-type heteropolytungstates.[9,10,15,16]

In the case of $K_8[\alpha_1\text{-}P_2W_{17}O_{61}Ru^{II}(DMSO)]$, four well-defined reversible redox pairs ($E_{1/2}$ = 1138, 357, −508, and −743 mV) are observed. The peak separations of the redox pairs at $E_{1/2}$ = 1138 and 357 mV are ca. 65 mV, indicating that these electrode processes are two reversible one-electron transfers[32] for $Ru^{IV/III}(DMSO)$ and $Ru^{III/II}(DMSO)$. The redox pairs at −508 and −743 mV are attributed to two two-electron reductions of the tungsten by comparing the peak current with the one-electron redox peak current.

In the case of $K_8[\alpha_2\text{-}P_2W_{17}O_{61}Ru^{II}(DMSO)]$, four well-defined reversible redox pairs ($E_{1/2}$ = 1148, 248, −462, and −632 mV) are observed. The peak separations of the redox pairs at $E_{1/2}$ = 1148 and 248 mV are ca. 78 and 68 mV, respectively, indicating that these electrode processes are two reversible one-electron transfers[32] for $Ru^{IV/III}(DMSO)$ and $Ru^{III/II}(DMSO)$. The redox pairs at −462 and −632 mV are attributed to two two-electron reductions of the tungsten by comparing the peak current with the one-electron redox peak current.

Figure 9 and Supporting Information Figure S8a,b show UV−vis spectra of $[\alpha_1\text{-}P_2W_{17}O_{61}Ru(DMSO)]^{n-}$ and $[\alpha_2\text{-}P_2W_{17}O_{61}Ru(DMSO)]^{n-}$ after electrolysis at potentials where $Ru^{III}(DMSO)$ species and $Ru^{II}(DMSO)$ species are produced. Both UV−vis spectra of $Ru^{II}(DMSO)$ species are slightly different from those of $[SiW_{11}O_{39}Ru^{II}(DMSO)]^{6-}$, $[GeW_{11}O_{39}Ru^{II}(DMSO)]^{6-}$, and $[PW_{11}O_{39}Ru^{II}(DMSO)]^{5-}$.[16]

Supporting Information Figure S8c,d shows the changes in absorbance of $[\alpha_1\text{-}P_2W_{17}O_{61}Ru(DMSO)]^{n-}$ and $[\alpha_2\text{-}P_2W_{17}O_{61}Ru(DMSO)]^{n-}$ in 0.5 M KH_2PO_4 (pH 4.3) at 480 nm against applied voltages. On the basis of these UV−vis

dx.doi.org/10.1021/ic403041s | Inorg. Chem. 2014, 53, 3526−3539

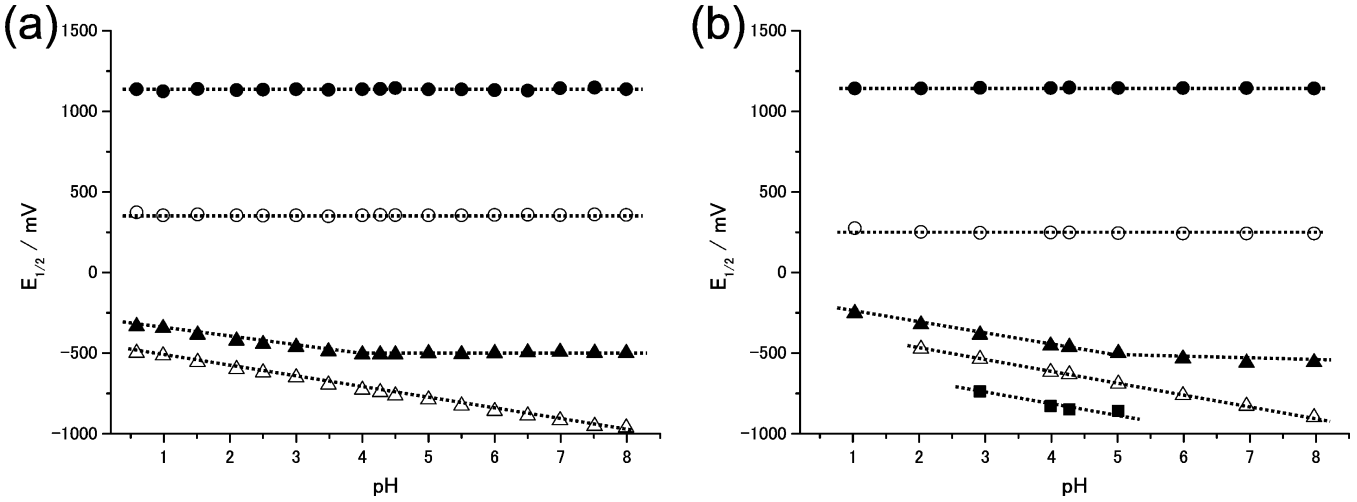

Figure 10. Pourbaix diagrams of (a) $K_8[\alpha_1\text{-}P_2W_{17}O_{61}Ru^{II}(DMSO)]$ and (b) $K_8[\alpha_2\text{-}P_2W_{17}O_{61}Ru^{II}(DMSO)]$. Redox potential $E_{1/2}$ for (●) $Ru^{IV/III}$, (○) $Ru^{III/II}$, (▲) first two-electron reduction, (△) second two-electron reduction, and (■) third two-electron reduction redox couples.

spectroelectrochemical measurements, the redox potentials of $Ru^{III/II}(DMSO)$ in $[\alpha_1\text{-}P_2W_{17}O_{61}Ru(DMSO)]^{n-}$ and $[\alpha_2\text{-}P_2W_{17}O_{61}Ru(DMSO)]^{n-}$ are estimated to be 357 and 248 mV, respectively, which are in good agreement with the redox potentials (357 and 248 mV) estimated by cyclic voltammetry.

Supporting Information Figure S9 shows CVs of $[\alpha_1\text{-}P_2W_{17}O_{61}Ru^{II}(DMSO)]^{8-}$ and $[\alpha_2\text{-}P_2W_{17}O_{61}Ru^{II}(DMSO)]^{8-}$ dissolved in phosphate solution with different pH values, and the redox potentials are plotted against the pH value of the solution (Figure 10). Both redox potentials of $Ru^{IV/III}(DMSO)$ and $Ru^{III/II}(DMSO)$ are independent of the pH value, indicating that these redox processes are not accompanied by protonation and deprotonation. Similar pH dependency is observed for redox potentials of $Ru^{IV/III}(DMSO)$ and $Ru^{III/II}(DMSO)$ of Ru(DMSO)-substituted α-Keggin-type heteropolytungstates.[9,15,16]

In the case of Ru(DMSO)-substituted α-Keggin-type phosphotungstate[9] and germanotungstate,[16] both the redox potentials of the two two-electron reductions of tungsten are accompanied by two proton protonations, and the first two-electron reductions are accompanied by two proton protonations in the pH ranges of 1−7 and 1−6, respectively (eq 6). Therefore, the redox potentials shift to more negative potential with a slope of ca. 59 mV/pH by increasing the pH of the solution.

$$[\alpha\text{-}XW_{11}O_{39}Ru^{II}(DMSO)]^{n-} + 2e^- + 2H^+ \rightleftharpoons H_2[\alpha\text{-}XW_{11}O_{39}Ru^{II}(DMSO)]^{n-}\ (X = P,\ n = 5,\ 1 < pH < 7;\ X = Ge,\ n = 6,\ 1 < pH < 6) \quad (6)$$

The redox potentials of two-electron reduction of tungsten of the both Ru(DMSO)-substituted Dawson-type phosphotungstates shift to more negative potential with a slope of ca. 59 mV/pH by increasing pH of the solution. However, the potential shifts of the first two-electron reduction are stopped at pH of ca. 4 and 5 for $[\alpha_1\text{-}P_2W_{17}O_{61}Ru^{II}(DMSO)]^{8-}$ and $[\alpha_2\text{-}P_2W_{17}O_{61}Ru^{II}(DMSO)]^{8-}$, respectively. When pH of the solution is further increased, the redox potentials are independent of pH of the solution (Figure 10). Furthermore, the first redox peak of the two-electron transfer starts to split into two one-electron transfers (Supporting Information Figure S9, eqs 7, 8, and 9). These results indicate that the reductions of tungsten are not accompanied by protonation in these pH ranges.

$$[\alpha_1\text{-}/\alpha_2\text{-}P_2W_{17}O_{61}Ru^{II}(DMSO)]^{8-} + 2e^- + 2H^+ \rightleftharpoons H_2[\alpha_1\text{-}/\alpha_2\text{-}P_2W_{17}O_{61}Ru^{II}(DMSO)]^{8-}\ (\alpha_1\text{-isomer},\ 1 < pH < \text{ca. } 4;\ \alpha_2\text{-isomer},\ 1 < pH < 5) \quad (7)$$

$$[\alpha_1\text{-}/\alpha_2\text{-}P_2W_{17}O_{61}Ru^{II}(DMSO)]^{8-} + e^- \rightleftharpoons [\alpha_1\text{-}/\alpha_2\text{-}P_2W_{17}O_{61}Ru^{II}(DMSO)]^{9-}\ (\alpha_1\text{-isomer},\ 4 < pH;\ \alpha_2\text{-isomer},\ 5 < pH) \quad (8)$$

$$[\alpha_1\text{-}/\alpha_2\text{-}P_2W_{17}O_{61}Ru^{II}(DMSO)]^{9-} + e^- \rightleftharpoons [\alpha_1\text{-}/\alpha_2\text{-}P_2W_{17}O_{61}Ru^{II}(DMSO)]^{10-}\ (\alpha_1\text{-isomer},\ 4 < pH;\ \alpha_2\text{-isomer},\ 5 < pH) \quad (9)$$

The redox potentials of $Ru^{IV/III}(DMSO)$ and $Ru^{III/II}(DMSO)$ in $[\alpha_1\text{-}P_2W_{17}O_{61}Ru(DMSO)]^{n-}$ and $[\alpha_2\text{-}P_2W_{17}O_{61}Ru(DMSO)]^{n-}$ are compared with those in α-Keggin-type derivatives (Table 2, Scheme 1). The redox potential of $[\alpha_1\text{-}P_2W_{17}O_{61}Ru^{III/II}(DMSO)]^{7/8-}$ is higher (ca. 110 mV) than that of $[\alpha_2\text{-}P_2W_{17}O_{61}Ru^{III/II}(DMSO)]^{7/8-}$, and these redox potentials are located between those of $[\alpha\text{-}PW_{11}O_{39}Ru^{III/II}(DMSO)]^{4/5-}$ and $[\alpha\text{-}GeW_{11}O_{39}Ru^{III/II}(DMSO)]^{5/6-}$. On the other hand, the redox potential of $[\alpha_1\text{-}P_2W_{17}O_{61}Ru^{IV/III}(DMSO)]^{6/7-}$ is slightly higher (ca. 10 mV) than that of $[\alpha_2\text{-}P_2W_{17}O_{61}Ru^{IV/III}(DMSO)]^{6/7-}$, and both are lower than that of $[\alpha\text{-}SiW_{11}O_{39}Ru^{IV/III}(DMSO)]^{4/5-}$.

There are some reports about comparison of redox potentials of metals (Co, Fe, Re, Os, Ce, and Tc) in α_1- and α_2-isomers of $[P_2W_{17}O_{61}M]^{n-}$. In the case of Tc=O-substituted Dawson-type phosphotungstates, the redox potential of the $Tc^{V/IV}$=O in the α_1-isomer is higher than that of the α_2-isomer,[44] whereas the opposite relation is observed in the case of Ce,[17] Co,[45] and Re=O[44]-containing compounds. In the case of Fe-substituted Dawson-type phosphotungstate, order of redox potentials of $Fe^{III/II}(H_2O)$ in the α_1-isomer and α_2-isomer depends on pH value of the solution.[46] In the case of Co-substituted Dawson-

dx.doi.org/10.1021/ic403041s | Inorg. Chem. 2014, 53, 3526−3539

Scheme 1. Comparison of Redox Potentials of Metals in Various Heteropolytungstates[a]

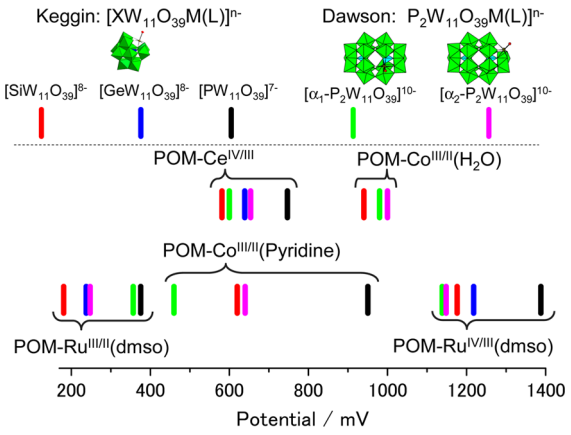

[a]Color bars represent redox potentials of metals in heteropolytungstates.

type phosphotungstate, the redox potential difference of $Co^{III/II}(L)$ between the α_1-isomer and α_2-isomer depends on the kind of ligand.[45] In general, redox potentials of metal incorporated in Keggin-type heteropolytungstates are in the order $[\alpha\text{-}PW_{11}O_{39}M(L)]^{n-} > [\alpha\text{-}GeW_{11}O_{39}M(L)]^{(n+1)-} > [\alpha\text{-}SiW_{11}O_{39}M(L)]^{(n+1)-}$, which could be explained by the difference of negative charge and electronegativity difference of Si and Ge. However, it is difficult to explain the redox potential of metal in a Dawson-type phosphotungstate, and further investigation to understand the redox potential including theoretical calculation is being planned.

CONCLUSION

Both α_1- and α_2-isomers of mono-Ru-substituted Dawson-type heteropolytungstates with DMSO as ligands, $[\alpha_1/\alpha_2\text{-}P_2W_{17}O_{61}Ru^{II}(DMSO)]^{8-}$, are isolated in pure form and are characterized using single-crystal X-ray structural analysis, IR, NMR, elemental analysis, mass spectroscopy, CV, and UV−vis. This is the first report of a mono-Ru-substituted Dawson-type heteropolytungstate being isolated in pure form with complete structural characterization. We clearly observed unusual isomerization from the α_2-isomer of a monolacunary Dawson-type phosphotungstate to its α_1-isomer.

Redox potential of the incorporated Ru is compared with those of Keggin-type derivatives, $[\alpha\text{-}XW_{11}O_{39}Ru(DMSO)]^{n-}$ (X = Si, Ge, or P). Redox potential of $Ru^{III/II}$ is in the order $[\alpha\text{-}PW_{11}O_{39}Ru^{III/II}(DMSO)]^{4/5-} > [\alpha_1\text{-}P_2W_{17}O_{61}Ru^{III/II}(DMSO)]^{7/8-} > [\alpha_2\text{-}P_2W_{17}O_{61}Ru^{III/II}(DMSO)]^{7/8-} > [\alpha\text{-}GeW_{11}O_{39}Ru^{III/II}(DMSO)]^{5/6-} > [\alpha\text{-}SiW_{11}O_{39}Ru^{III/II}(DMSO)]^{5/6-}$. Further investigation to understand their redox properties is being planned.

The α_1-isomer is an enantiomer, though it exists now as a racemic mixture, and has a potential as an enantioselective catalyst. Mono-Ru-substituted heteropolytungstates are active catalysts for several oxidation and reduction reactions. Hasenknopf, Thorimbert, and Lacôte's group reported enantiomer separation of the α_1-isomer of an Sn-substituted Dawson-type phosphotungstate using its reactivity difference with a peptide.[19] It is possible to react Ru with several organic compounds,[12,15,16,47] and further investigation for separation of redox active enantiomers is now underway in our group.

ASSOCIATED CONTENT

Supporting Information

Figure S1−S9 and Scheme S1 containing ^1H and ^{31}P NMR, UV−vis, CV, redox potential comparison, and ESI-MS spectra. Crystallographic data in CIF format. This material is available free of charge via the Internet at http://pubs.acs.org.

AUTHOR INFORMATION

Corresponding Author

*E-mail: sadakane09@hiroshima-u.ac.jp. Fax: +81 82 424 5494. Phone: +81 82 424 4456.

Notes

The authors declare no competing financial interest.

ACKNOWLEDGMENTS

This research was supported by the JST, PRESTO program. The synchrotron radiation experiments were performed at the BL02B1 and BL40XU of SPring-8 with the approval of the Japan Synchrotron Radiation Research Institute (JASRI) (Proposals 2012B1109 and 2012B1110). X-ray diffraction analysis was made using Bruker APEX Ultra, at the Natural Science Center for Basic Research and Development (N-BARD), Hiroshima University. We thank Mr. H. Fujitaka and Ms. T. Amimoto (N-BARD) for the measurements of ^{183}W NMR and ESI-MS, respectively.

REFERENCES

(1) Long, D. L.; Tsunashima, R.; Cronin, L. *Angew. Chem., Int. Ed.* **2010**, *49*, 1736.
(2) Special Thematic Issue on Polyoxometalates: Hill, C. L. *Chem. Rev.* **1998**, *98*, 1.
(3) Special Thematic Issue on Polyoxometalates: Cronin, L. *Chem. Soc. Rev.* **2012**, *41*, 7325.
(4) Putaj, P.; Lefebvre, F. *Coord. Chem. Rev.* **2011**, *255*, 1642.
(5) Izarova, N. V.; Pope, M. T.; Kortz, U. *Angew. Chem., Int. Ed.* **2012**, *51*, 9492.
(6) Bagno, A.; Bonchio, M.; Sartorel, A.; Scorrano, G. *Eur. J. Inorg. Chem.* **2000**, 17.
(7) Murakami, M.; Hong, D.; Suenobu, T.; Yamaguchi, S.; Ogura, T.; Fukuzumi, S. *J. Am. Chem. Soc.* **2011**, *133*, 11605.
(8) Ogo, S.; Miyamoto, M.; Ide, Y.; Sano, T.; Sadakane, M. *Dalton Trans.* **2012**, *41*, 9901.
(9) Sadakane, M.; Rinn, N.; Moroi, S.; Kitatomi, H.; Ozeki, T.; Kurasawa, M.; Itakura, M.; Hayakawa, S.; Kato, K.; Miyamoto, M.; Ogo, S.; Ide, Y.; Sano, T. *Z. Anorg. Allg. Chem.* **2011**, *637*, 1467.
(10) Yokoyama, A.; Ohkubo, K.; Ishizuka, T.; Kojima, T.; Fukuzumi, S. *Dalton Trans.* **2012**, *41*, 10006.
(11) Bart, J. C.; Anson, F. C. *J. Electroanal. Chem.* **1995**, *390*, 11.
(12) Rong, C.; Pope, M. T. *J. Am. Chem. Soc.* **1992**, *114*, 2932.
(13) Khenkin, A. M.; Efremenko, I.; Weiner, L.; Martin, J. M. L.; Neumann, R. *Chem.—Eur. J.* **2010**, *16*, 1356.
(14) Sadakane, M.; Higashijima, M. *Dalton Trans.* **2003**, 659.
(15) Sadakane, M.; Tsukuma, D.; Dickman, M. H.; Bassil, B.; Kortz, U.; Higashijima, M.; Ueda, W. *Dalton Trans.* **2006**, 4271.
(16) Ogo, S.; Shimizu, N.; Ozeki, T.; Kobayashi, Y.; Ide, Y.; Sano, T.; Sadakane, M. *Dalton Trans.* **2013**, *42*, 2540.
(17) Sadakane, M.; Dickman, M. H.; Pope, M. T. *Inorg. Chem.* **2001**, *40*, 2715.
(18) Boglio, C.; Hasenknopf, B.; Lenoble, G.; Rémy, P.; Gouzerh, P.; Thrimbert, S.; Lacôte, E.; Malacria, M.; Thouvenot, R. *Chem.—Eur. J.* **2008**, *14*, 1532.
(19) Micoine, K.; Hasenknopf, B.; Thorimbert, S.; Lacôte, E.; Malacria, M. *Angew. Chem., Int. Ed.* **2009**, *48*, 3466.
(20) Nomiya, K.; Torii, H.; Nomura, K.; Sato, Y. *J. Chem. Soc., Dalton Trans.* **2001**, 1506.

(21) Evans, I. P.; Spencer, A.; Wilkinson, G. *J. Chem. Soc., Dalton Trans.* **1973**, 204.
(22) Contant, R.; Klemperer, W. G.; Yaghi, O. *Inorg. Synth.* **1990**, *27*, 104.
(23) Sheldrick, G. M. *Acta Crystallogr.* **2007**, *A64*, 112.
(24) Sheldrick, G. M. *SADABS*; University of Göttingen: Göttingen, Germany, 1996.
(25) Yasuda, N.; Fukuyama, Y.; Toriumi, K.; Kimura, S.; Takata, M. *AIP Conf. Proc.* **2010**, *1234*, 147.
(26) Yasuda, N.; Murayama, H.; Fukuyama, Y.; Kim, J.; Kimura, S.; Toriumi, K.; Tanaka, Y.; Moritomo, Y.; Kuroiwa, Y.; Kato, K.; Tanaka, H.; Takata, M. *J. Synchrotron Radiat.* **2009**, *16*, 352.
(27) Sheldrick, G. M. *SHELXS-97*; University of Göttingen: Göttingen, Germany, 1997.
(28) Graham, C. R.; Finke, R. G. *Inorg. Chem.* **2008**, *47*, 3679.
(29) Sakai, Y.; Shinohara, A.; Hayashi, K.; Nomiya, K. *Eur. J. Inorg. Chem.* **2006**, 163.
(30) Sadakane, M.; Ostuni, A.; Pope, M. T. *J. Chem. Soc., Dalton Trans.* **2002**, 63.
(31) Artero, V.; Lahootun, V.; Villanneau, R.; Thouvenot, R.; Herson, P.; Gouzerh, P.; Proust, A. *Inorg. Chem.* **2005**, *44*, 2826.
(32) Bard, A. J.; Faulkner, L. R. *Electrochemical Methods*; Wiley: New York, 1980.
(33) Toth, J. E.; Anson, F. C. *J. Electroanal. Chem.* **1988**, *256*, 361.
(34) Himeno, S.; Takamoto, M.; Ueda, T. *J. Electoanal. Chem.* **2000**, *485*, 49.
(35) Sadakane, M.; Steckhan, E. *J. Mol. Catal. A: Chem.* **1996**, *114*, 221.
(36) Contant, R.; Abbessi, M.; Canny, J.; Belhouari, A.; Keita, B.; Nadjo, L. *Inorg. Chem.* **1997**, *36*, 4961.
(37) Jennings, W. B. *Chem. Rev.* **1975**, *75*, 307.
(38) Dablemont, C.; Hamaker, C. G.; Thouvenot, R.; Sojka, Z.; Che, M.; Maatta, E. A.; Proust, A. *Chem.—Eur. J.* **2006**, *12*, 9150.
(39) Bi, L.-H.; Kortz, U.; Keita, B.; Nadjo, L. *Dalton Trans.* **2004**, 3182.
(40) Laurencin, D.; Proust, A.; Gérard, H. *Inorg. Chem.* **2008**, *47*, 7888.
(41) Laurencin, D.; Villanneau, R.; Gérard, H.; Proust, A. *J. Phys. Chem. A* **2006**, *110*, 6345.
(42) Laurencin, D.; Thouvenot, R.; Boubekeur, K.; Gouzerh, P.; Proust, A. *C. R. Chim.* **2012**, *15*, 135.
(43) Shimizu, N.; Ozeki, T.; Shikama, H.; Sano, T.; Sadakane, M. *J. Cluster. Sci.* DOI: 10.1007/s10876-013-0641-9.
(44) McGregor, D.; Burton-Pye, B. P.; Mbomekallé, I. M.; Aparicio, P. A.; Romo, S.; López, X.; Poblet, J. M.; Francesconi, L. C. *Inorg. Chem.* **2012**, *51*, 9017.
(45) Samonte, J. L.; Pope, M. T. *Can. J. Chem.* **2001**, *79*, 802.
(46) Vilà, N.; Aparicio, P. A.; Sécheresse, F.; Poblet, J. M.; López, X.; Mbomekallé, I. M. *Inorg. Chem.* **2012**, *51*, 6129.
(47) Sadakane, M.; Moroi, S.; Iimuro, Y.; Izarova, N.; Kortz, U.; Hayakawa, S.; Kato, K.; Ogo, S.; Ide, Y.; Ueda, W.; Sano, T. *Chem.—Asian J.* **2012**, *7*, 1331.